

University of Dundee

Numerical analysis of collapse in a deep excavation supported by ground anchors

Baziar, Mohammad Hassan; Ghadamgahi, Alireza; Brennan, Andrew John

Published in:

Proceedings of the Institution of Civil Engineers: Geotechnical Engineering

DOI:

[10.1680/jgeen.19.00122](https://doi.org/10.1680/jgeen.19.00122)

Publication date:

2021

Document Version

Peer reviewed version

[Link to publication in Discovery Research Portal](#)

Citation for published version (APA):

Baziar, M. H., Ghadamgahi, A., & Brennan, A. J. (2021). Numerical analysis of collapse in a deep excavation supported by ground anchors. *Proceedings of the Institution of Civil Engineers: Geotechnical Engineering*, 174(3), 263-278. <https://doi.org/10.1680/jgeen.19.00122>

General rights

Copyright and moral rights for the publications made accessible in Discovery Research Portal are retained by the authors and/or other copyright owners and it is a condition of accessing publications that users recognise and abide by the legal requirements associated with these rights.

- Users may download and print one copy of any publication from Discovery Research Portal for the purpose of private study or research.
- You may not further distribute the material or use it for any profit-making activity or commercial gain.
- You may freely distribute the URL identifying the publication in the public portal.

Take down policy

If you believe that this document breaches copyright please contact us providing details, and we will remove access to the work immediately and investigate your claim.

Geotechnical Engineering

Numerical analysis of collapse in a deep excavation supported by ground anchors

--Manuscript Draft--

Manuscript Number:	GE-D-19-00122R3
Full Title:	Numerical analysis of collapse in a deep excavation supported by ground anchors
Article Type:	Paper of 3000-5000 words in length
Corresponding Author:	Mohammad Hassan Baziar, PhD Iran University of Science & Technology (IUST) Tehran, IRAN (ISLAMIC REPUBLIC OF)
Corresponding Author Secondary Information:	
Corresponding Author's Institution:	Iran University of Science & Technology (IUST)
Corresponding Author's Secondary Institution:	
First Author:	Mohammad Hassan Baziar, PhD
First Author Secondary Information:	
Order of Authors:	Mohammad Hassan Baziar, PhD Alireza Ghadamgahi, PhD student Andrew John Brennan, PhD
Order of Authors Secondary Information:	
Abstract:	<p>On October 3, 2013, a global failure occurred in one of the stabilized sections of a deep excavation in Shahrak-e gharb in Tehran. The excavation supported by ground anchors with enlarge reinforced concrete thrust blocks and sprayed concrete facing. The failure occurred despite the system passing conventional limit equilibrium design and satisfying requirements in terms of allowable displacements. This work aims firstly to model the case of Shahrak-e gharb using ABAQUS in order to understand the soil deformation leading to the failure condition. It is shown that a near-surface zone of weaker fill material was responsible for the failure. As displacements during construction and soil failure mechanisms are well matched in the numerical model, the case study is then considered to be a validation case for the numerical model, and a parametric study is performed on the extent to which anchoring bypasses the weaker surface soil. This shows that a proper embedment into the competent soils is important, as excessive strains can still develop if the anchor bond zone is insufficiently confined, potentially leading to progressive collapse.</p>
Additional Information:	
Question	Response
Please enter the number of total words in your abstract, main text and references.	6927
Please enter the number of figures, photographs and tables in your submission.	18 figures 3 tables
Funding Information:	

Numerical analysis of collapse in a deep excavation supported by ground anchors

Author 1

Mohammad Hassan Baziar, Professor

School of Civil Engineering, Iran University of Science and Technology, Tehran, Iran

Author 2

Alireza Ghadamgahi, PhD student

School of Civil Engineering, Iran University of Science and Technology, Tehran, Iran

Author 3

Andrew John Brennan, Senior Lecturer

Civil Engineering Division, School of Science and Engineering, University of Dundee, Dundee, UK

Contact details of corresponding author:

Email: baziar@iust.ac.ir

Tell: +9821-73228110

Address: School of Civil Engineering, Iran University of Science and Technology, Narmak, Tehran

16765163, Islamic Republic of Iran

Abstract

On October 3, 2013, a global failure occurred in one of the stabilized sections of a deep excavation in Shahrak-e gharb in Tehran. The excavation supported by ground anchors with enlarge reinforced concrete thrust blocks and sprayed concrete facing. The failure occurred despite the system passing conventional limit equilibrium design and satisfying requirements in terms of allowable displacements. This work aims firstly to model the case of Shahrak-e gharb using ABAQUS in order to understand the soil deformation leading to the failure condition. It is shown that a near-surface zone of weaker fill material was responsible for the failure. As displacements during construction and soil failure mechanisms are well matched in the numerical model, the case study is then considered to be a validation case for the numerical model, and a parametric study is performed on the extent to which anchoring bypasses the weaker surface soil. This shows that a proper embedment into the competent soils is important, as excessive strains can still develop if the anchor bond zone is insufficiently confined, potentially leading to progressive collapse.

Keywords: failure; excavation; anchors & anchorages

1. Introduction

Soil nail and ground anchored systems, respectively classified as passive and active anchorages, are efficient stabilization techniques for slopes and excavations and have been widely used throughout the world over the past three decades. Ground anchored walls, also referred to as “tieback walls”, can be a better method when a structure, sensitive to soil movement, exists near the excavation walls (Lazarte et al., 2015). This method involves the use of prestressed grouted ground anchors as structural elements that transmit applied tensile loads into the ground. The basic components of a grouted ground anchor, including the anchor head, the unbonded length, and the bond length, are presented in Figure 1.

The majority of research on stabilized slopes and excavations has focused on soil nail systems, using both physical model tests (e.g., Tei et al., 1998; Zhang et al., 2001; Hong et al., 2005; Zhang et al., 2013) and numerical studies (e.g., Smith and Su, 1997; Fan and Luo, 2008; Wei and Cheng 2010; Razavi and Hajjalilue Bonab 2017). There are also some studies in which the behavior of ground anchored systems has been investigated. Briaud and Lim (1999) conducted numerical modeling to study the effect of various design decisions for a 7.5 m tieback wall. The numerical model was calibrated against an instrumented case history. Their results provided some information about the impact of the anchor forces, the location of the anchor unbonded zone, the stiffness of the wood lagging, and the embedment of the soldier piles on the wall behavior. Finno and Roboski (2005) studied 3D ground deformations of a 12.8 m tieback excavation in which the support was provided by a sheet pile wall and three levels of ground anchors. A performance-based relationship as a function of safety factor against basal heave and excavation depth was proposed for the estimation of lateral ground displacement. Their empirical method was presented to predict the distribution of ground deformations parallel to the excavation wall. Kim et al. (2007) proposed a finite element method and a beam-column method to study the load transfer mechanism of ground anchors. Their numerical results were compared with field

measurements. It was reported that both methods could provide reasonable predictions on the load-displacement behavior of ground anchors.

The main purpose of most of these research works has been to study the effect of various components on the stability of the soil nail and ground anchored retaining systems, while the serviceability and deformation behavior of these retaining walls have received less attention. Furthermore, conventional soil nail reference manuals (e.g., Lazarte et al., 2015) and also ground anchored systems guides (e.g., Sabatini et al., 1999), which are based on limit equilibrium methods, recommend just a simple equation as a function of wall height for the allowable displacements and provide little information about predicting the movement of these walls. Consequently, designers often conduct numerical simulations to estimate the wall movements. However, using the maximum lateral displacement as the outcome of the numerical analysis and its comparison with the allowable displacement cannot always make a comprehensive picture of the wall behavior. This is because the performance of ground anchored walls is significantly influenced by their complex interaction with soils. Furthermore, other factors, such as the grout injection method, the type of vertical support, the connection between the anchor head and the bond zone, the presence of weak soil layers, are also likely to affect the behavior of ground anchored walls. There is, therefore, a need for rigorous investigation regarding the effect of each component on the ground anchored wall performance.

In this research, a finite element procedure is proposed for deformation analysis of a deep post-grouted ground anchored excavation. Special attention is given to the precise simulation of contact interactions between the reinforcing elements and the surrounding soil. To verify the proposed numerical model, the computed deformations are compared with the measured lateral displacements of a case study ground anchored wall. Utilizing this verified FE model, the following issues are investigated. First, the reason behind the collapse that occurred in one of the sections of this case is discussed. Following this, the efficiency of the service limit state requirements for ground anchored excavations is investigated by

comparing the maximum predicted displacement with the allowable value. Then, a true distance between the bond zone of the uppermost anchors and the top fill layer is explored, particularly an extent to which the anchoring mechanism does not develop excessive strain around the embedded area of the anchors.

2. Case study background

On 3 October 2013, a failure occurred in one section of a deep excavation project known as Iran-zamin Excavation, located in the Shahrak-e gharb in the heart of Tehran, the capital of Iran. As shown in Figure 2(a), the project site had a triangle-shaped plan with an area of 16000 m². The target excavation depth was planned to be 40 m.

2.1. Design considerations

To stabilize the excavation walls, a ground anchor system, including post-grouted ground anchors supported by reinforced concrete blocks, was employed (S.E.S. Consulting & Contracting Co., 2013). In this method, as can be seen in Figure 3(a), reinforced concrete blocks, located just behind each anchor head, were used rather than more conventional vertical connectors, e.g., soldier beams (Figure 3(b)) or sheet-piles.

In this project, the excavation support system was designed for short-term conditions with the allowable stress design approach given in FHWA (Sabatini et al., 1999). The safety factor against overall stability was checked to be at least 1.35 using limit equilibrium analysis by Geo-Slope software. The ultimate displacement of the excavation walls was limited up to 0.005H, where H represents the wall height. Numerical modeling was also carried out using PLAXIS software to evaluate maximum displacements (S.E.S. Consulting & Contracting Co., 2013).

As shown in Figure 2(a), the design of the support system was divided into 14 sections with similar stratification and height, named North-1, North-2, etc. A bond length of 6 m was considered for post-grouted ground anchors. The anchors were composed of six 15-mm-diameter steel strands having an ultimate strength of 260 kN. Using multiple high strength steel strand, provided the possibility of defining a design prestress load of 900 kN to achieve an adequate safety factor against overall stability and also reducing the lateral displacements of the excavation walls (S.E.S. Consulting & Contracting Co., 2013). The mechanical properties of the ground anchors, including bond length and unbonded length, are shown in Table 1. Just behind each anchor head, a cast-in-place reinforced concrete block was planned to transmit anchor prestress load to the soil mass and also to prevent punching shear of the anchor head. These blocks were designed like an isolated footing with length, width, and thickness of 1.2 m, 1.2 m, and 0.45 m, respectively. Moreover, a 100-mm-thick layer of reinforced shotcrete facing was used to keep the soil from weathering and surficial failure (S.E.S. Consulting & Contracting Co., 2013). The mechanical parameters of the reinforced concrete blocks and facing are also presented in Table 1.

2.2. Subsoil conditions

In terms of general geology, the project region represents the distribution of the Pliocene and Quaternary alluvial deposits in Tehran plain. Tehran alluvium formations are divided into four groups: A (Hezardarreh formation), B (Kahrizak formation), C (Tehran Alluvial formation), and D (Recent Alluvium). The main characteristics of Tehran alluvium formations are given in Table 2 (Sharifzadeh et al., 2013). The project region contained A formation in the middle, northern and western areas of the site while it contained younger C formation underlain by A formation in the southern and eastern areas (Z.S.A. Consulting Co., 2012).

To investigate underground conditions, nine boreholes (BH-1 to BH-9) were sunk to depths between 50 m and 97 m. Besides, two 5.5-m-deep and 7.5-m-deep trial pits were excavated (Z.S.A. Consulting Co., 2012). Figure 2(a) shows the positions of the various boreholes and trial pits in the project plan. Detailed information from all the boreholes located on the site is presented in Figures 4 and 5. Figure 4 shows the profiles of the SPT-N values, fines, sand, and gravel contents with depth. As shown in Figure 4(a), the N values exceed more than 50 from depths of 4 m toward the end of boreholes, although there are some fluctuations until a depth of approximately 10 m below the ground surface. Figure 4(b) illustrates that the fine contents range from 20% to 80%, with more distributions below 50%. As shown in Figures 4(c) and (d), the coarse material mostly consists of sand. Figure 5 shows the distribution of moisture contents together with Atterberg limits and plasticity index with depth. The moisture contents range from 3% to 23%, and the liquid limits range between 29% and 48%, which indicates that the fine material in this site had low plasticity. The plasticity index is in the range of 10% to 28% showing that the fine contents are mainly from clay material. Site investigations revealed the existence of weak fill material at the top of soil profiles, with a variable depth between 4 m and 8.5 m in different sections. This is a common soil layer for many nearly developed areas in Tehran, where extensive leveling has resulted in a thick fill layer. The distribution of the fill layer in different sections is shown in Figure 2(b). Deeper soils below the fill layer were largely composed of dense to very dense clayey sand with gravel (SC), with more than 20% clay, and very stiff to hard lean clay with sand (LC) (Z.S.A. Consulting Co., 2012).

In terms of subsurface water conditions, geotechnical exploration and GPR (Ground Penetration Radar) tests showed only some local perched water zones at different depth surrounding the site. A dewatering and drainage system, including some deep vertical wells and prefabricated vertical drains behind the shotcrete facing, was designed to remove any risk induced by underground water (Z.S.A. Consulting Co., 2012).

To determine the shear strength parameters of the subsoil, an in situ direct shear test and several sets of lab direct shear tests and triaxial tests were carried out during the site investigation. The in situ direct shear test, which was conducted at the bottom of trial pit 2, showed a cohesion of $c'=24$ kPa and a friction angle of $\phi'=40.8$ for the clayey sand. According to the result of lab tests, the cohesion ranged from 0 to 30 kPa, and the friction angle ranged between 22.9° and 42° (Z.S.A. Consulting Co., 2012).

2.3. Construction method

The excavation support system was constructed in some main construction phases. Each phase was corresponding to an excavation lift. To stabilize the unsupported cut following each excavation lift, a staged-construction method was performed. Using the ODEX method, several 147-mm-diameter holes at an angle of 10° or 13° with respect to the horizontal plane were drilled into the excavated face to install the ground anchors. Parsapajouh et al., (2012) described the detail of installing the post-grouted anchors. Subsequently, a square opening, surrounding each anchor head, was dug down for each reinforced concrete block (Figure 3(a)) and followed by placing a special rebar mesh. After installing timber formwork and reinforcing bars, the openings were filled with concrete, and then the excavated face was covered with a 100-mm-thick reinforced concrete layer utilizing the shotcrete technique. At the final stage, following installing the bearing plate, the prestress load of each anchor was applied.

2.4. The behavior of ground anchored excavation walls

As shown in Figure 2(a), 14 monitoring sections (named NP1, NP2, ..., WP1, and so on) were planned in this project. In each monitoring section, from 2 to 5 points on the wall face (in total, more than 50 points) were monitored using survey equipment during the construction. The construction had been carried out for 12 months without incident. However, in early October 2013, when the section North-2 was being excavated at a depth of approximately 32 m, the lateral displacement of this section substantially increased, ending in global collapse. Figure 6 illustrates the wall failure had an extent of 18

1
2
3
4 138 m down the face of the wall (Figure 6(a)) and 12 m perpendicular to the wall (Figure 6(b)). Figure 7
5
6 139 shows some cracks, induced by such failure, on the neighboring buildings located in the north of the
7
8
9 140 collapsed section. After the wall failure, it was observed that the depth of fill soil layer around this
10
11 141 section was approximately 10 m rather than 6.8 m used in the design process. Figure 8 indicates the
12
13
14 142 stratification of section North-2, based on the site investigation as well as the post-collapse
15
16 143 observations. The properties of each soil layer used in the design of the excavation support system are
17
18 144 shown in Table 3. The reliability of these values was again confirmed through further site investigations
19
20
21 145 conducted after the collapse.

22
23
24 146 In this section, ten rows of ground anchors had been used, all of which had a lock-off load of 900 kN.
25
26 147 The first row of anchors was inclined at 13° with respect to the horizontal plane, and the other rows
27
28
29 148 were inclined at 10° . Figure 8 shows the schematic positions of the ground anchors and their unbonded
30
31 149 length for the same section. The vertical distance between the head of the ground anchors is also shown
32
33 150 in Figure 8. The horizontal distance between the ground anchors in the first row, in the second to the
34
35
36 151 ninth rows, and in the tenth row were 3.1 m, 3.4 m, and 1.8 m, respectively. In the design of section
37
38 152 North-2, the computed factor of safety against overall stability was predicted to be 1.371, and the
39
40 153 maximum lateral and vertical displacement were estimated to be 57 mm and 62 mm, respectively (S.E.S.
41
42
43 154 Consulting & Contracting Co., 2013). The predicted values, including safety factor and maximum
44
45 155 displacements, had satisfied the requirements specified by FHWA (Sabatini et al., 1999).

46
47
48 156 Despite the collapse in section North-2, most of the other wall sections showed a sensible and safe
49
50
51 157 performance during construction. Monitoring results of section North-4, which was undamaged, is used
52
53 158 as a part of validation assessment for the following numerical simulation. In this section, all ten rows of
54
55
56 159 ground anchors had a prestress load of 900 kN and were inclined at 10° with respect to the horizontal
57
58 160 plane. The unbonded length of ground anchors and the vertical distance between the anchors head are
59
60 161 shown in Figure 9(a). The horizontal distance between ground anchors in the first nine rows was 3.4 m
61
62
63
64
65

1
2
3
4 162 while it was 1.8 m in the tenth row (lower row). Figure 9(a) also shows the thickness of different soil
5
6 163 layers in section North-4, where the fill soil layer had a depth of 4.3 m. In the design process of section
7
8
9 164 North-4, the computed factor of safety against overall stability was predicted to be 1.456, and the
10
11 165 maximum lateral and vertical displacement were estimated to be 51 mm and 61 mm, respectively (S.E.S.
12
13
14 166 Consulting & Contracting Co., 2013). All the predicted values had satisfied the requirements specified by
15
16 167 FHWA (Sabatini et al., 1999). Figure 9(b) shows that this section had a height of 31 m in which lateral
17
18 168 displacements at three points (NPA, NPB, and NPC), located at a distance of 1.5 m, 4.4 m and 16.3 m
19
20
21 169 below the crest of the wall, respectively, were monitored.

22
23
24 170 In the design process, all the wall sections were predicted to be safe, while global collapse occurred in
25
26 171 one of the sections. Therefore, the current study is further conducted to explore the actual reason for
27
28
29 172 the collapse, utilizing the finite element method. This case study can further help to explore the effect of
30
31 173 different system variables.

3. Numerical modeling of the post-grouted ground anchored walls

34
35
36 174
37
38 175 The behavior of the anchor-stabilized walls is investigated using a stress-deformation analysis. The
39
40 176 construction sequence of post-grouted ground anchored walls, as well as contact interactions between
41
42 177 reinforcing elements surfaces and the surrounding soil, are dominant factors which can affect the result
43
44
45 178 of a numerical analysis. In this study, a numerical analysis procedure is conducted to reasonably cover
46
47 179 these issues.

3.1. Finite element modeling

50
51 180
52
53 181 The two wall sections studied in the current study are long enough and far from the corners of the site
54
55 182 plan. Due to the satisfaction of the plane strain condition, a 2D numerical model is adopted to perform
56
57
58 183 the numerical analysis using the ABAQUS software. The motivation for employing this software is its
59
60 184 successful results, obtained in various geotechnical issues (Helwany, 2007) especially numerical

simulation of soil-nailed slopes (Zhou et al., 2009), ground anchored slopes (Kim et al., 2013) and ground anchored walls (Briaud and Lim, 1999). Moreover, the connection between model components has a significant effect on the result of numerical simulation, and ABAQUS is able to accurately simulate discrete elements of a model (Hibbitt et al., 2016).

In the present study, soil and concrete blocks are simulated by the homogeneous solid section, facing is modeled using the beam section, and ground anchors are simulated by the truss section. The properties of the reinforcing elements and soil layers (Table 1 and Table 3) have been used to specify the section characteristics in numerical modeling. The linear-elastic behavior is used for the ground anchors, the reinforced concrete blocks, and the facing in the numerical modeling. The Mohr-Coulomb constitutive model using non-associated flow rule is employed for the surrounding soil. This model is believed to be suitable since the system is largely governed by frictional failure, and also it has been previously used for similar subjects (Kim et al., 2013). The parameters of the Mohr-Coulomb model are Young's modulus (E'), and Poisson's ratio (ν) for soil elasticity; angle of shearing resistance (ϕ'), and cohesion (c') for soil plasticity, and angle of dilation (ψ).

The FE mesh used in the analysis is shown in Figure 10. The mesh pattern is symmetrically designated for the left and right sides of the wall face. A relatively fine mesh is used in the zone of anchors, and the mesh size becomes coarser farther from the reinforced area. The four-node bilinear plane strain quadrilateral element, known as CPE4, with full integration is used to mesh the soil and the concrete blocks. The two-node linear two-dimensional truss element (T2D2) and the two-node linear beam in a plane element (B21) are employed to mesh the anchor bond length and the facing, respectively.

As is shown in Figure 10, the distance from the right and left boundaries to the wall face are chosen $2H$, where H is the height of the wall. The bottom boundary is selected at a distance of H from the excavation subgrade. Kim et al., (2013) employed similar distances for the side and bottom boundaries

to study the stability of a ground-anchored slope using finite element modeling. These dimensions are assumed to be adequate to eliminate the boundary effects on the wall performance. The side boundaries are constrained against the horizontal movement while the bottom boundary is constrained against the horizontal and vertical movements.

3.2. Numerical procedure for simulating the interaction between reinforcing elements and surrounding soil

In practice, the bond zone in post-grouted ground anchors is performed using multiple grout injections under high-pressure to enlarge the grout body of straight-shafted gravity grouted ground anchors. Due to this installation method, there would be no distinctive interface between the anchor bond zone and the surrounding soil, as shown in Figure 11(b). To properly model this, any slippage on the interface between these two components should be restricted in numerical modeling. The embedded-region constraint, which allows a part of the model to be embedded within a host area of the model, is employed to confine anchor bond length inside the soil. As a result, the translational degrees of freedom of the embedded elements (anchor bond zone) are constrained to the surrounding soil, and the reinforcement mechanism of post-grouted anchors is appropriately simulated.

As can be seen in Figures 1 and 11, the unbonded length is that portion of the prestressed steel that is free to elastically elongate and transfer the resisting force from the bond length to the structure (Sabatini et al., 1999). Therefore, if a one-dimensional linear elastic relationship between the anchor head (point “A” in Figure 11(b)) and the beginning point of anchor bond length (point “B” in Figure 11(b)) is developed, it can simulate the real performance of the anchor unbonded length. This idea is performed in a three-stage process throughout the FE modeling. First, a virtual wire is created between points A and B, and these points are defined as the reference points. Following this, one transitional degree of freedom along the wire is established utilizing the axial connector. The process culminates with specifying the linear elastic behavior between points A and B along the wire.

The reinforced concrete blocks do not slide relative to soil surfaces because these blocks are placed inside the cut. The tie constraint is used to constrain the blocks into the soil. The use of this type of constraint permits two separate surfaces to be fused together to avoid any relative movement between them.

Finally, based on the performed construction method of facing, it is assumed that relative movement between the facing and the adjacent soil does not take place. Thus, the interface between the shotcrete facing and the soil is described as perfectly rough by implementing the embedded-region constraint, which can accurately model beam elements (like facing) lying embedded in solid elements.

3.3. Numerical procedure of stress-deformation analysis

The stress-deformation analysis, including the construction sequence of ground anchored walls, is performed to obtain the wall movements. The numerical techniques for simulating interactions between the reinforcing elements and the surrounding soil, described in the previous section, are implemented in the FE modeling. The following steps, as shown in Figure 12, are required for the stress-deformation analysis:

Step1: The 2D FE mesh, including the ground anchors, facing, and reinforced concrete blocks, is generated. The whole excavation zone is divided into ten partitions corresponding to the real construction phases (excavation lifts) in the field (Figure 12(a)). The depth of the excavation lifts is 1m below the elevation where the relevant row of anchors is installed. These elevations were presented earlier in Figures 8 and 9(a) for sections North-2 and North-4, respectively.

Step 2: The natural condition of ground layers is modeled by deactivation of all the reinforcing elements. The properties of soil layers are assigned, and the boundary conditions are applied to the model (Figure 12(b)).

Step 3: The initial ground stresses are applied to the FE model using the geostatic analysis procedure in which in situ stresses are generated without any deformation (Figure 12(c)).

Step 4: The first layer of soil, corresponding to the initial excavation lift, is removed (Figure 12(d)).

Step 5: The relevant reinforcing elements of the current phase, including the bond length of the ground anchor, the reinforced concrete block, and the facing, are activated with their material properties. The interaction between the reinforcing element and the soil is generated. During this step, the gravity forces are applied to the new reinforcing elements added to the system (Figure 12(e)).

Step 6: The simulated feature for modeling the anchor unbonded length is generated (Figure 12(f)).

Step 7: The prestress load of the related anchor is applied along the wire between the first reference point (anchor head), and the second reference point (starting point of the anchor bond length), (Figure 12(g)).

Step 8: The stress-deformation analysis is performed. This step experiences the static-general analysis procedure in which changes in stress and corresponding displacements are produced (Figure 12(h)).

As the ground anchored support system was constructed in ten excavation phases, steps 4-8 of the above are repeated ten times to obtain the wall deformation at the end of each construction phase. This approach provides the possibility of comparing numerical results with those measured in the site at the end of each construction phase.

4. Result of numerical analyses

4.1. Comparing field data with computed results

The measured lateral wall displacements at the end of the construction phases for three points in section North-4 (Figure 9(b)) are compared with those computed in Figure 13. In this figure, the outward

1
2
3
4 274 wall movements are shown with negative quantities. The observed lateral displacements of point NPA at
5
6 275 the end of construction phases as well as the numerical results are presented in Figure 13(a). Since
7
8
9 276 monitoring of point NPA was started at the end of the third construction phase, the field deformations
10
11 277 are compared with the numerical data from this phase. Comparison of the field lateral displacements of
12
13
14 278 point NPB as well as their computed results are shown in Figure 13(b). Similarly, this point was
15
16 279 monitored from the end of phase 3, so both the measured data and the predicted movements are
17
18 280 presented from this phase. As is shown, the calculated values for both NPA and NPB are in good
19
20
21 281 agreement with the recorded data except those lateral displacements that are computed at the end of
22
23 282 the third and fourth steps. The computed lateral displacements of both NPA and NPB, at the end of the
24
25 283 third and fourth phases, predict a slight inward movement. This movement is due to the huge prestress
26
27
28 284 loads applied to the anchors at each phase, causing the points close to the crest of the wall (like NPA
29
30 285 and NPB) to show marginal inward movements, as long as the excavated depth is less than about 12 m
31
32
33 286 (end of step 4).

34
35
36 287 Figure 13(c) draws a comparison between the recorded lateral displacements of point NPC and the
37
38 288 computed results. As monitoring of point NPC was begun at the end of phase 6, the comparison is
39
40 289 illustrated from this phase. The calculated lateral movements at various construction phases agree well
41
42
43 290 with the measured data with the predicted values slightly higher than the displacement monitored in
44
45 291 the site.

4.2. Numerical simulation of the collapse

46
47
48 292
49
50 293 To simulate the wall behavior in section North-2, the depth of the top soil layer has been modified
51
52
53 294 according to the in situ observation after the collapse. Figure 14 indicates the contours of computed
54
55 295 lateral displacement following complete construction. The deformed shape of the wall face due to
56
57
58 296 lateral movements is also presented in Figure 14. As is shown, a maximum lateral movement of 103 mm
59
60
61
62
63
64
65

is predicted in the middle of the wall height (at the base of the fill soil layer). Besides, a significant lateral displacement of about 70 mm can be seen around the bond zone of the two top rows of ground anchors located in the top soil layer of fill material. The predicted wall deformations are less than the allowable limit (160 mm). However, failure still occurred, suggesting that judging the stability of a deep ground anchored wall by just comparing the numerically predicted displacement with the allowable value may be insufficient as a comprehensive assessment of the wall serviceability. In this study, the potential failure surfaces are located where the greatest total strain occurs. Figure 15 illustrates two developed failure surfaces from the maximum total strain distribution plot. The first surface is located in the bond zone of two top anchors, extending toward the lower anchors and the ground surface. This interior failure surface seems to play a significant role in the expansion of the second failure surface, located close to the wall facing. When this shallow failure surface is noticed, it can be seen that the computed depth of failure surface is 18.1 m compared to the depth of 18 m measured on the site, and the predicted breadth of the failure surface is 11.5 m compared to the measured 12 m, which gives confidence that the FE model is capable of properly modeling the observed failure. To draw a clear reason for the collapse, based on numerical analysis, it can be concluded that since the bond length of two top anchors were placed in the weaker fill soil layer, when the excavation reached to a depth of 32 m they failed to transfer the developed bond stress into the soil. This is because the load of anchors at the excavated depth of 32 m had increased to more than their initial lock-off load. Thus, these anchors were pulled out of the soil, and a large lateral displacement was created in their bond zone, leading to a shallow failure.

4.3. Effect of top fill layer on the occurrence of failure

Since the numerical model has matched the observed failure as well as the recorded wall displacements during the construction phases, it is a suitable model for further investigation. If the depth of fill soil layer around section North-2 had been accurately estimated, the occurred failure would have been

avoided. This is particularly important for the areas where past activities have created a thick layer of loose fill material near the ground surface. Thus, this section aims to discuss what kind of considerations should be taken into account concerning the position of bond zone of the uppermost anchor to reach an adequate level of serviceability when a thick loose fill layer exists at the top of the soil profile. Accordingly, the following six models are considered. Model 1 represents the section North-2 in which the depth of the fill layer is modeled based on the initial estimation in the original design of the ground anchored excavation. In this model, all the ground anchors are located in competent soil. However, the vertical distance between the center of the uppermost anchor bond zone and the fill layer, d , is approximately 1.6 m. Figure 16(a) indicates the position of the bond zone of the uppermost anchor in Model 1. To evaluate the effect of “ d ” on the wall behavior, this distance is increased in the next models. Such an increase is performed by enlarging the unbonded length of the anchor, with an increment of 1 m, while keeping all other parameters constant. Figure 16(b) illustrates Model 6, in which “ d ” is increased to 2.8 m.

Figure 17 shows the lateral wall displacements of all six models as a function of wall height. As can be seen, a maximum lateral movement of 66 mm, which takes place in the middle third of the wall height, is predicted for Model 1. This value is less than the allowable limit, and the wall is assumed to have an acceptable serviceability level. To determine possible failure conditions, the result of the maximum total strain distribution in Model 1 is presented in Figure 18(a). As is shown, a partial failure surface can be distinguished behind the bond zone of the uppermost anchor, developing to the two lower anchors and also the ground surface. This observation confirms that the potential failure surfaces may not be detected using predicted deformations during wall design. In addition, if Figure 18(a) is compared with Figure 15, it can further support the idea that the interior failure surface has an important effect on the formation of the shallow failure surface. In other words, it can be concluded that the occurred failure

was progressive collapse starting from the bond zone of two top ground anchors and then led to the shallow collapse.

More attention in Figure 17 indicates that when “d” increases from 1.6 m (in Model 1) to 2.8 m (in Model 6), the maximum lateral wall movement experiences a marginal decline of 7 mm. At first glance, such an increase in the magnitude of “d” may be regarded unimportant. However, a comparison between the maximum total strain contour plots in Models 1, 4, and 6 (Figures 18(a)-(c), respectively) reveals that such an increase for “d” causes gradual elimination of any potential interior failure surfaces. If Model 1 is compared with Model 6, it can be seen that the strain values have experienced a moderate decrease and the local failure surface behind the bond zone of the uppermost anchor has been perfectly removed. As a result, although the predicted value of maximum displacement in Model 1 meets the requirement limit, to eliminate any partial failure surface that may lead to progressive collapse, it is recommended that the uppermost anchors bypass the top fill layer into the competent soil to the extent that anchoring mechanisms no longer cause excessive strain around the embedded area of the anchors.

5. Conclusion

The following findings can be drawn from the current study:

1. It was found out that the wall failure was progressive collapse starting from the bond zone of two top rows of ground anchors located in the top soil layer of fill material.
2. Stress-deformation analyses revealed the possibility of the collapse for two following circumstances: actual soil layer conditions after the collapse and soil layer conditions based on the initial subsurface investigation. However, the maximum displacements in both cases, obtained by numerical modeling, satisfied the allowable limit, $0.005H$. Thus, meeting this requirement cannot always guarantee the wall serviceability.

3. Studying the distribution of generated maximum total strains in the soil surrounding the anchor bond zone can be regarded as a further desirable criterion for analyzing the performance of post-grouted ground anchored walls. This is because such observation can exhibit the potential local failure surfaces in weaker soils where anchoring mechanisms may develop excessive strain around the embedded area of the anchors.

4. In the case of the existence of a thick layer of fill material at the top of the soil profile, the embedment of the bond zone of the uppermost anchors into the competent soil can reduce the maximum lateral wall displacement, while this might not be sufficient by itself for the safe wall performance. The uppermost anchors should be adequately confined into the competent soil to the extent that eradicates local failure from the confined area that can lead to progressive collapse. For a 6.8-m-thick fill layer at the top of the soil profile, increasing the vertical distance between the bond zone of the uppermost anchor and the top fill layer by 1.2 m (from 1.6 m to 2.8 m) could eliminate the cause of concern of any local failure.

5. Unlike the passive ground anchored walls in which the maximum lateral deformation takes place at the top of the wall, for a deep ground anchored wall (32 m high) supported by active reinforcement systems, the peak movement was observed in the middle third of the wall height. This issue is specifically crucial when critical points need to be selected for the performance-monitoring plan during the wall construction.

6. In the design process of the ground anchored walls, wall deformations are considered as service limit states. These limit states refer to the conditions which do not involve collapse. This case shows that wall movements may be the primary design issue (strength limit state) for an excavation support system located in a major urban area. Besides, more experimental and numerical works should be performed to investigate the tolerable deformation limits for deep ground anchored walls.

1
2
3
4
5
6
7
8
9
10
11
12
13
14
15
16
17
18
19
20
21
22
23
24
25
26
27
28
29
30
31
32
33
34
35
36
37
38
39
40
41
42
43
44
45
46
47
48
49
50
51
52
53
54
55
56
57
58
59
60
61
62
63
64
65

6. Acknowledgment

The support of Dr. Siavash Litkouhi, Senior Manager at SES Co., and Dr. Ali Nabizadeh, former Board Member of Tehran Construction Engineering Organization, for providing the detailed information of the Iran-zamin case, are appreciated.

References

- Briaud, J. L., & Lim, Y. (1999). Tieback walls in sand: numerical simulation and design implications. *Journal of geotechnical and geoenvironmental engineering*, 125(2), 101-110.
- Fan, C. C., & Luo, J. H. (2008). Numerical study on the optimum layout of soil-nailed slopes. *Computers and Geotechnics*, 35(4), 585-599.
- Finno, R. J., & Roboski, J. F. (2005). Three-dimensional responses of a tied-back excavation through clay. *Journal of Geotechnical and Geoenvironmental Engineering*, 131(3), 273-282.
- Helwany, S. (2007). *Applied soil mechanics with ABAQUS applications*. John Wiley & Sons.
- Hibbitt, H., Karlsson, B., & Sorensen, P. (2016). *Abaqus Analysis User's Manual Version 2016*. Dassault Systèmes Simulia Corp, Providence.
- Hong, Y. S., Chen, R. H., Wu, C. S., & Chen, J. R. (2005). Shaking table tests and stability analysis of steep nailed slopes. *Canadian Geotechnical Journal*, 42(5), 1264-1279.
- Kim, N. K., Park, J. S., & Kim, S. K. (2007). Numerical simulation of ground anchors. *Computers and Geotechnics*, 34(6), 498-507.
- Kim, Y., Lee, S., Jeong, S., & Kim, J. (2013). The effect of pressure-grouted soil nails on the stability of weathered soil slopes. *Computers and Geotechnics*, 49, 253-263.
- Lazarte, C. A., Robinson, H., Gómez, J. E., Baxter, A., Cadden, A., & Berg, R. (2015). *Soil Nail Walls Reference Manual (No. FHWA-NHI-14-007)*.
- Parsapajouh, A., Litkouhi, S., & Amini, B. (2012). A Case Study on Excavation Stabilization Using Ground Anchors and High-Pressure Injection. In *Grouting and Deep Mixing 2012* (pp. 1115-1123).
- Razavi, S. K., & Hajialilue Bonab, M. (2017). Study of soil nailed wall under service loading condition. *Proceedings of the Institution of Civil Engineers-Geotechnical Engineering*, 170(2), 161-174.
- S.E.S. Consulting & Contracting Co., (2013). *Design Report for Iran-Zamin Excavation Project*, Report 19.
- Sabatini, P. J., Pass, D. G., & Bachus, R. C. (1999). *Geotechnical engineering circular no. 4: ground anchors and anchored systems (No. FHWA-IF-99-015)*.
- Sharifzadeh, M., Kolivand, F., Ghorbani, M., & Yasrobi, S. (2013). Design of sequential excavation method for large span urban tunnels in soft ground–Niayesh tunnel. *Tunnelling and Underground Space Technology*, 35, 178-188.

1
2
3
4 Smith, I. M., & Su, N. (1997). Three-dimensional FE analysis of a nailed soil wall curved in
5 plan. *International Journal for Numerical and Analytical Methods in Geomechanics*, 21(9), 583-597.
6

7
8 Tei, K., TAYLOR, N. R., & Milligan, G. W. (1998). Centrifuge model tests of nailed soil slopes. *Soils and*
9 *foundations*, 38(2), 165-177.
10

11
12 Wei, W. B., & Cheng, Y. M. (2010). Soil nailed slope by strength reduction and limit equilibrium
13 methods. *Computers and Geotechnics*, 37(5), 602-618.
14

15
16 Z.S.A. Consulting Co., (2012). *Geotechnical Investigations & Foundation Report for Iran-Zamin Excavation*
17 *Project*.
18

19
20 Zhang, G., Cao, J., & Wang, L. (2013). Centrifuge model tests of deformation and failure of nailing-
21 reinforced slope under vertical surface loading conditions. *Soils and Foundations*, 53(1), 117-129.
22

23
24 Zhang, J., Pu, J., Zhang, M., & Qiu, T. (2001). Model tests by centrifuge of soil nail
25 reinforcements. *Journal of testing and evaluation*, 29(4), 315-328.
26

27
28 Zhou, Y. D., Cheuk, C. Y., & Tham, L. G. (2009). An embedded bond-slip model for finite element
29 modelling of soil–nail interaction. *Computers and Geotechnics*, 36(6), 1090-1097.
30
31
32
33
34
35
36
37
38
39
40
41
42
43
44
45
46
47
48
49
50
51
52
53
54
55
56
57
58
59
60
61
62
63
64
65

1
2
3
4 **List of Tables**
5

6 Table 1. Properties of reinforcing elements (S.E.S. Consulting & Contracting Co., 2013)
7

8 Table 2. Geological characteristics of the alluvium formations in Tehran (Sharifzadeh et al., 2013)
9

10 Table 3. Geotechnical parameters of soil layers used in design (S.E.S. Consulting & Contracting Co., 2013)
11
12
13
14
15
16
17
18
19
20
21
22
23
24
25
26
27
28
29
30
31
32
33
34
35
36
37
38
39
40
41
42
43
44
45
46
47
48
49
50
51
52
53
54
55
56
57
58
59
60
61
62
63
64
65

List of Figures

Figure 1. Components of a ground anchor

Figure 2. Site plan: (a) the position of various design and monitoring sections and the geotechnical investigations boreholes; (b) depth of the fill layer at the various sections

Figure 3. Two types of shallow support that is used during construction of ground anchored walls: (a) cast-in-place reinforced concrete block (this case); (b) cast-in-place concrete pile as soldier beam

Figure 4. Information from borehole logs: (a) SPT-N; (b) fine content; (c) sand content; and (d) gravel content

Figure 5. Information from borehole logs: (a) moisture content; (b) plastic limit; (c) liquid limit; and (d) plastic index

Figure 6. Dimensions of failure mass: (a) depth of failure; (b) width of failure

Figure 7. The failure-induced cracks: (a) adjacent wall; (b) back of the collapsed wall; (c); and (d) surrounding buildings

Figure 8. Schematic view of section North-2: (a) stratification based on the initial site investigation; (b) real stratification based on the initial site investigation and the post-collapse observations

Figure 9. Schematic view of section North-4: (a) stratification and vertical location of the ground anchors; (b) location of the monitoring points

Figure 10. The 2D FE mesh for the ground anchored wall and the boundary conditions

Figure 11. Schematic view of different anchor types: (a) gravity grouted anchors; (b) post-grouted anchors

Figure 12. Numerical procedure of stress-deformation analysis for a post-grouted ground anchored wall: (a) step 1, (b) step 2, (c) step 3, (d) step 4, (e) step 5, (f) step 6, (g) step 7, and (h) step 8

Figure 13. Comparison between the field lateral displacements and the computed results at the end of construction phases for three points in section North-4 (Monitoring section NP2)

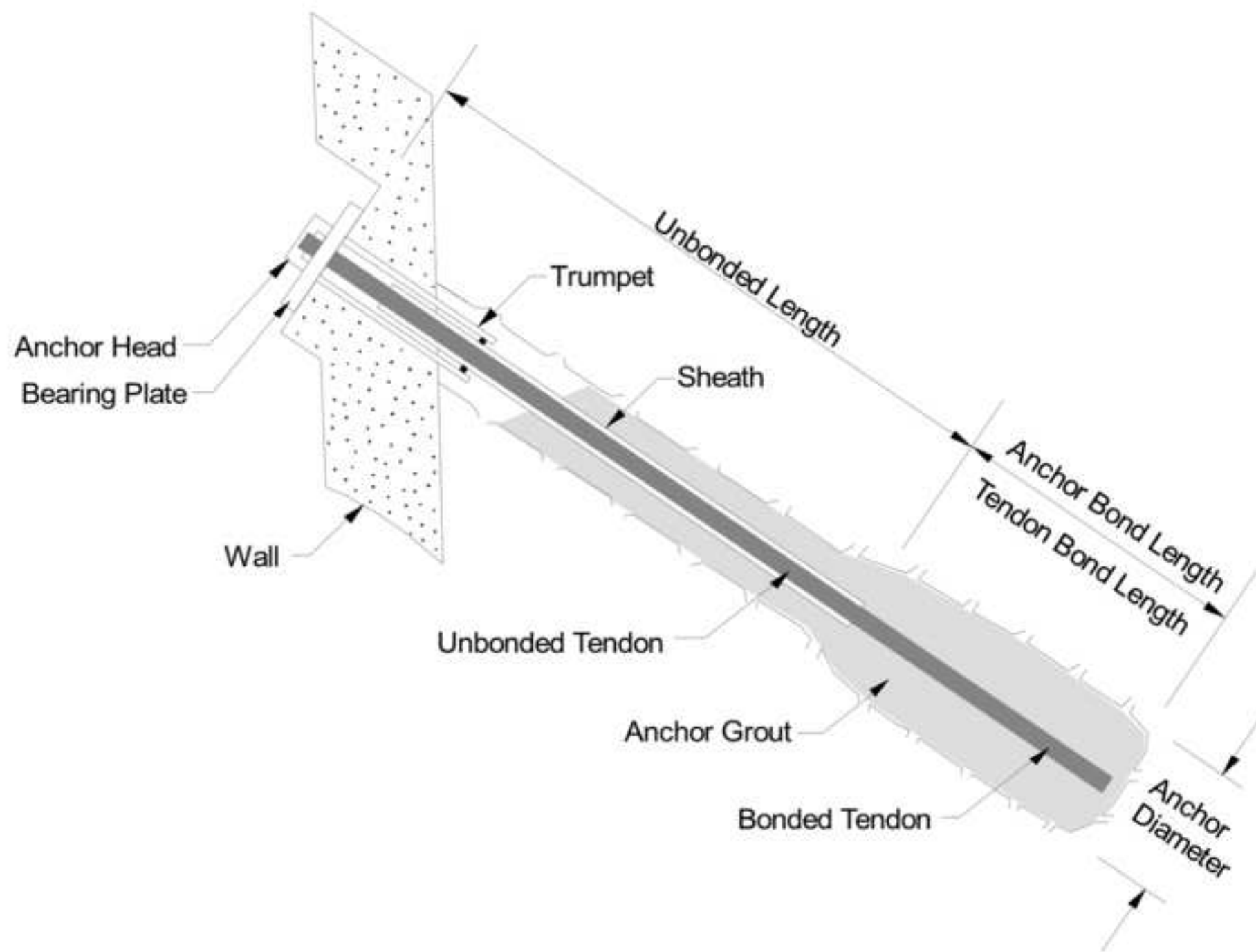
Figure 14. Distribution of the computed lateral displacement in section North-2

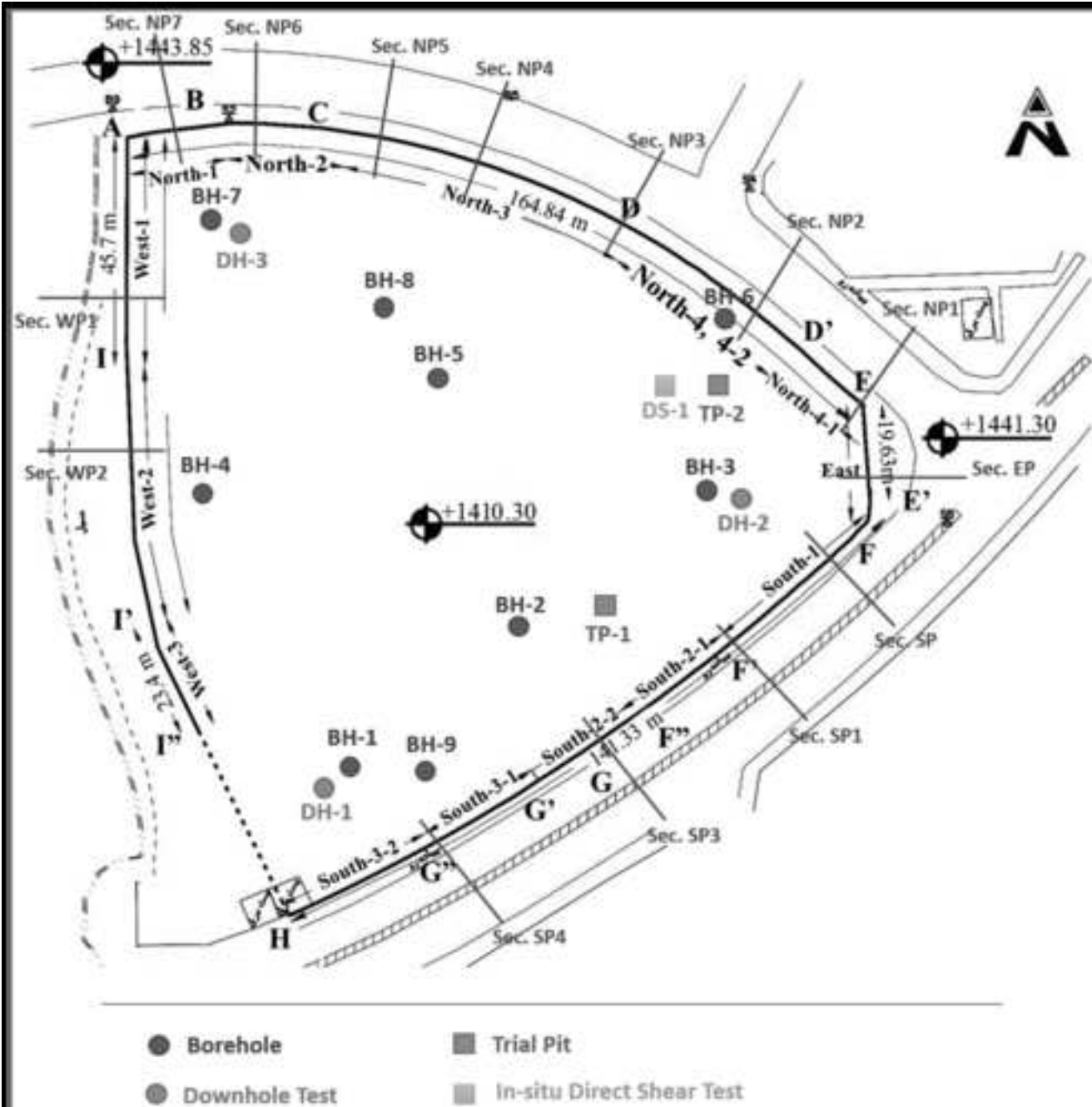
Figure 15. Distribution of the computed maximum total strain and depiction of failure surfaces in section North-2

Figure 16. Position of the bond length of the uppermost anchor from the top fill layer

Figure 17. The computed lateral wall deformation as a function of wall height for different Models

Figure 18. Distribution of the computed maximum total strain and depiction of interior failure surface behind the bond zone of the uppermost anchor: (a) Model 1, (b) Model 4, and (c) Model 6

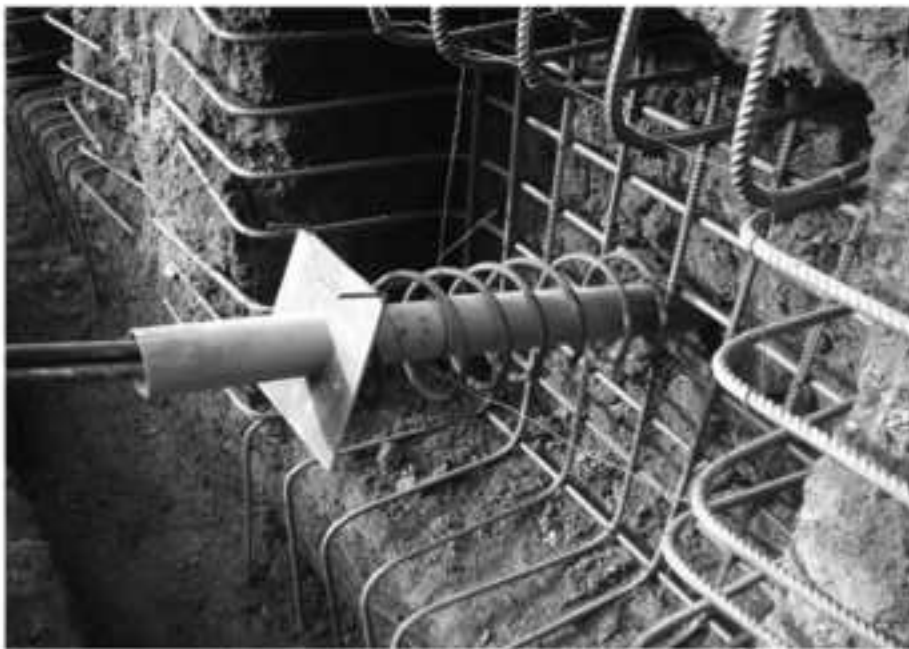




(a)

Section No.	Section Name	Depth of fill layer (m)
1	North-1	7.3
2	North-2	6.8
3	North-3	6.5
4	North-4, 4-2	4.3
5	North-4-1	4.0
6	East	4.0
7	South-1	5.0
8	South-2-1	5.1
9	South-2-2	5.1
10	South-3-1	8.1
11	South-3-2	8.1
12	West-1	8.5
13	West-2	5.0
14	West-3	5.7

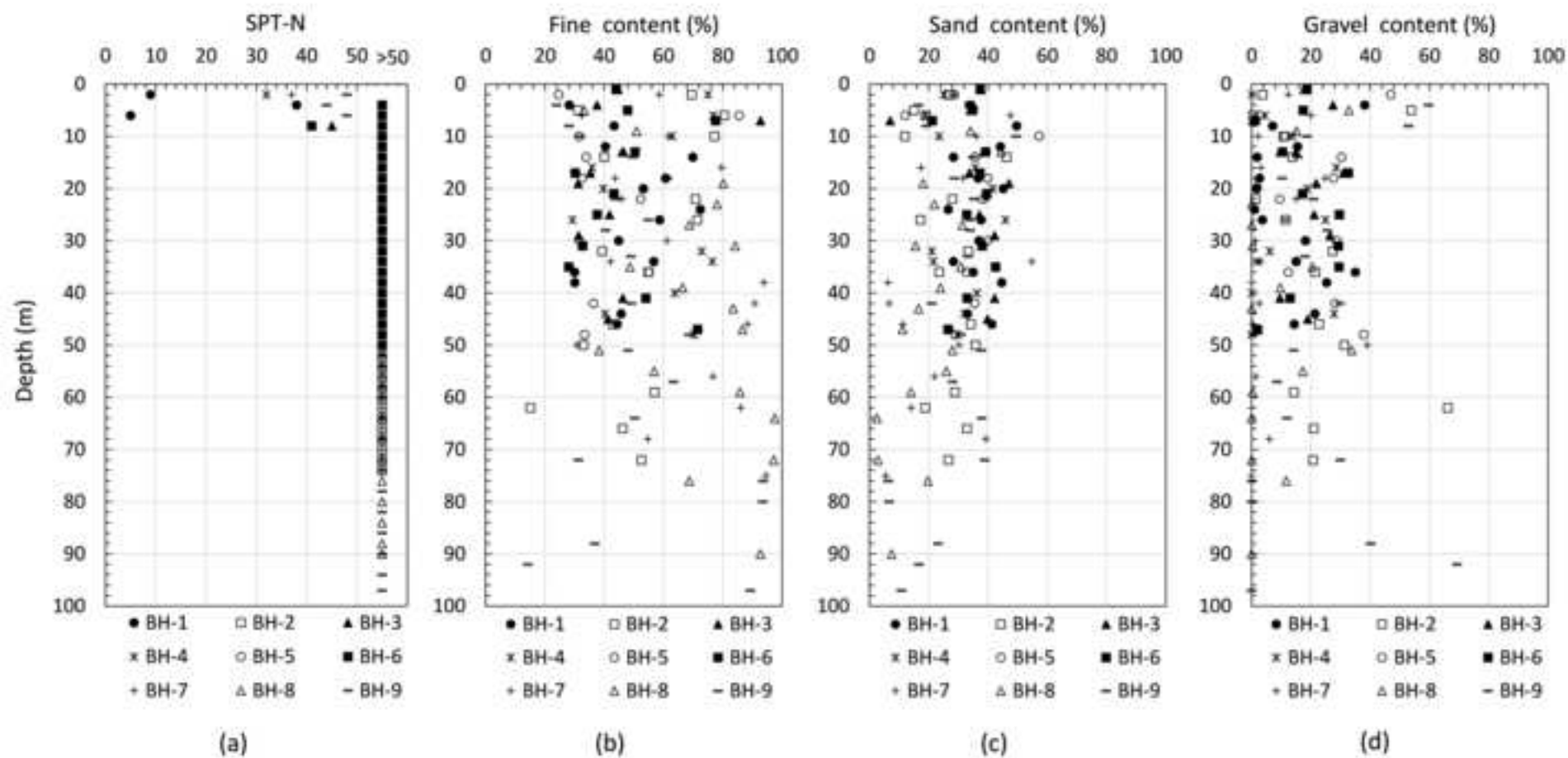
(b)

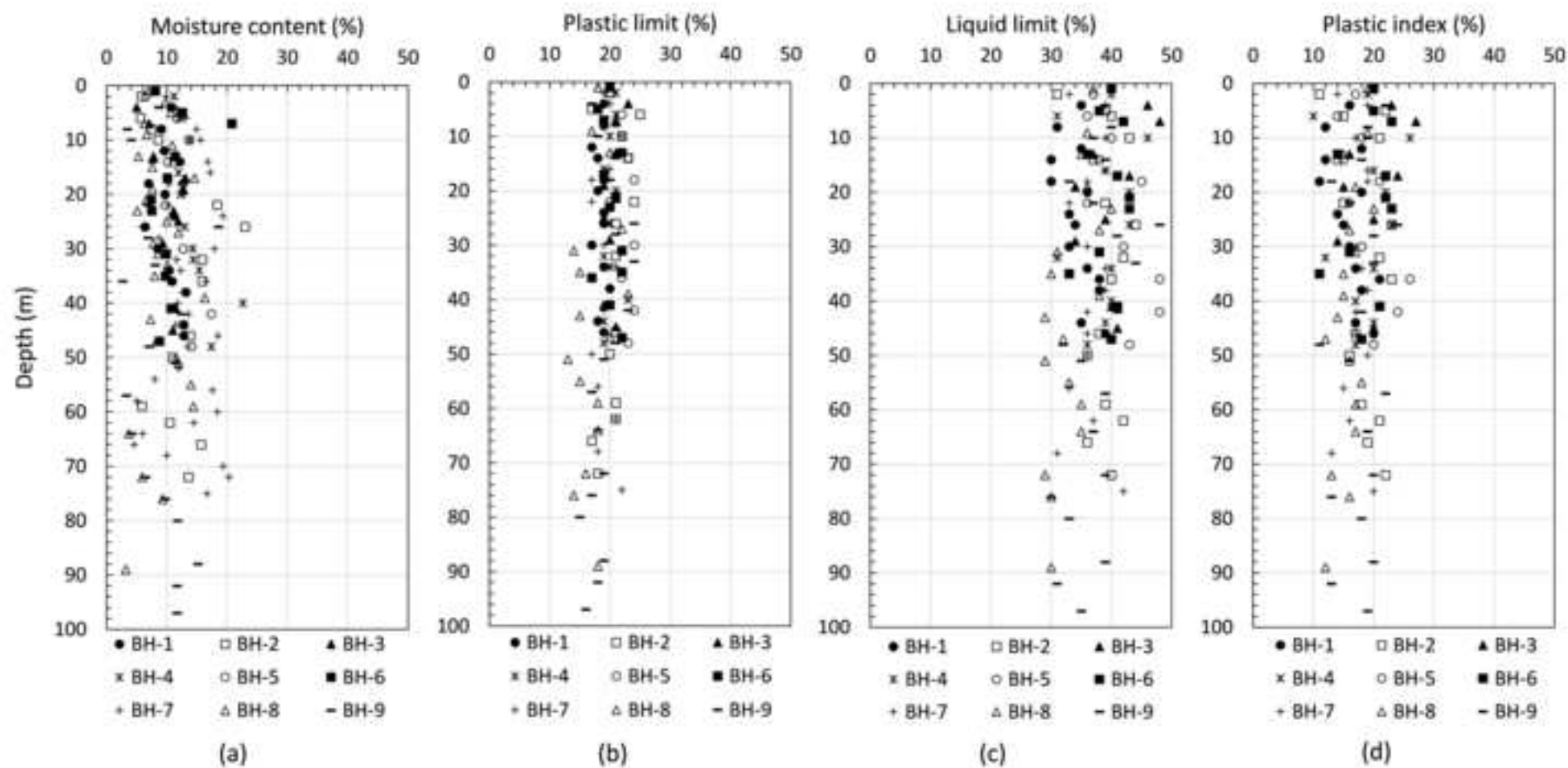


(a)



(b)







(a)



(b)



(a)



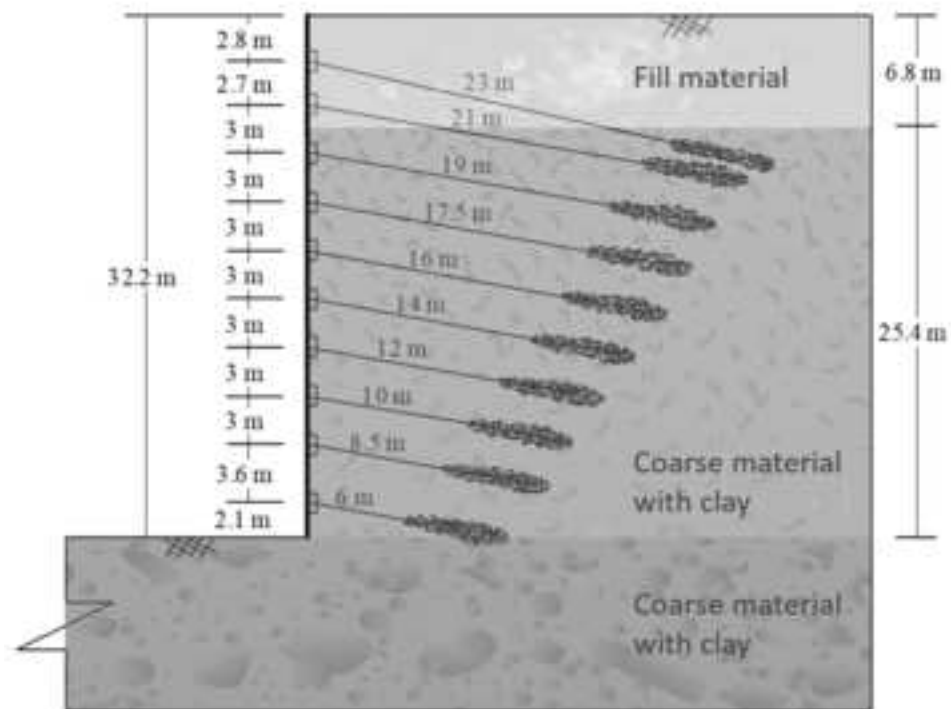
(b)



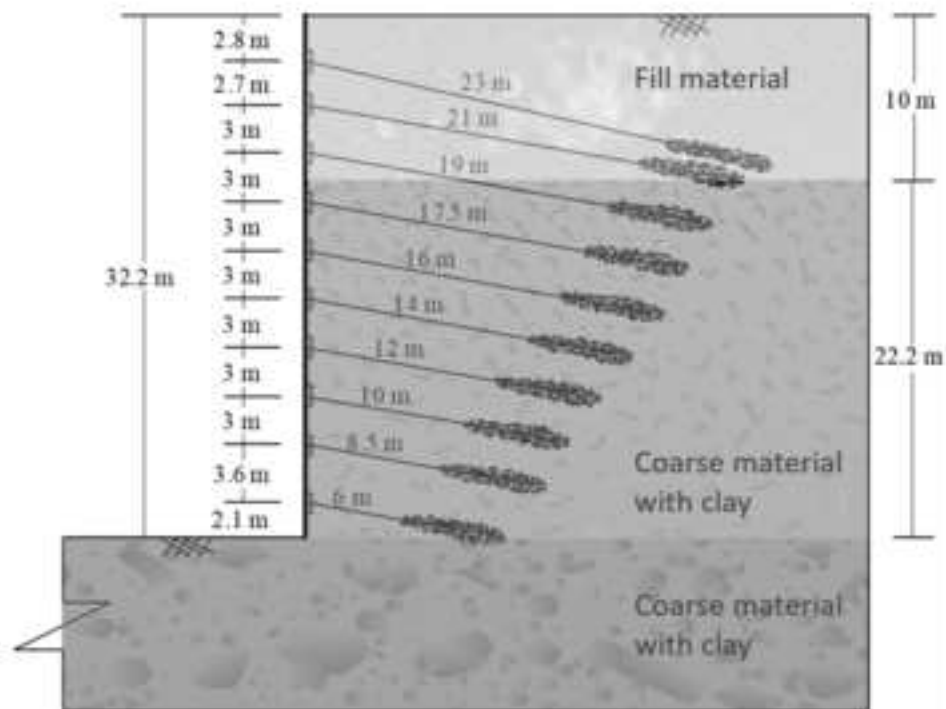
(c)



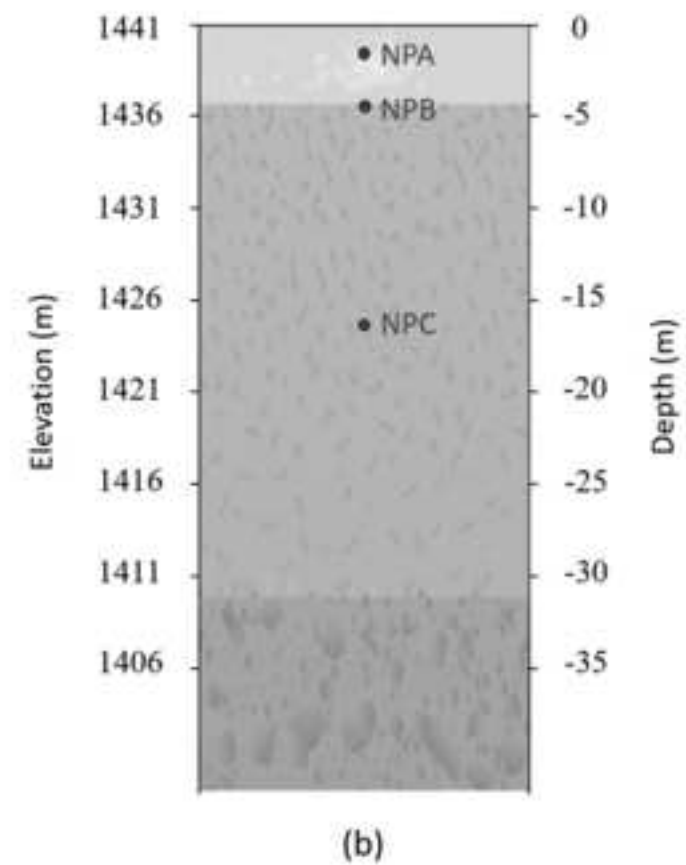
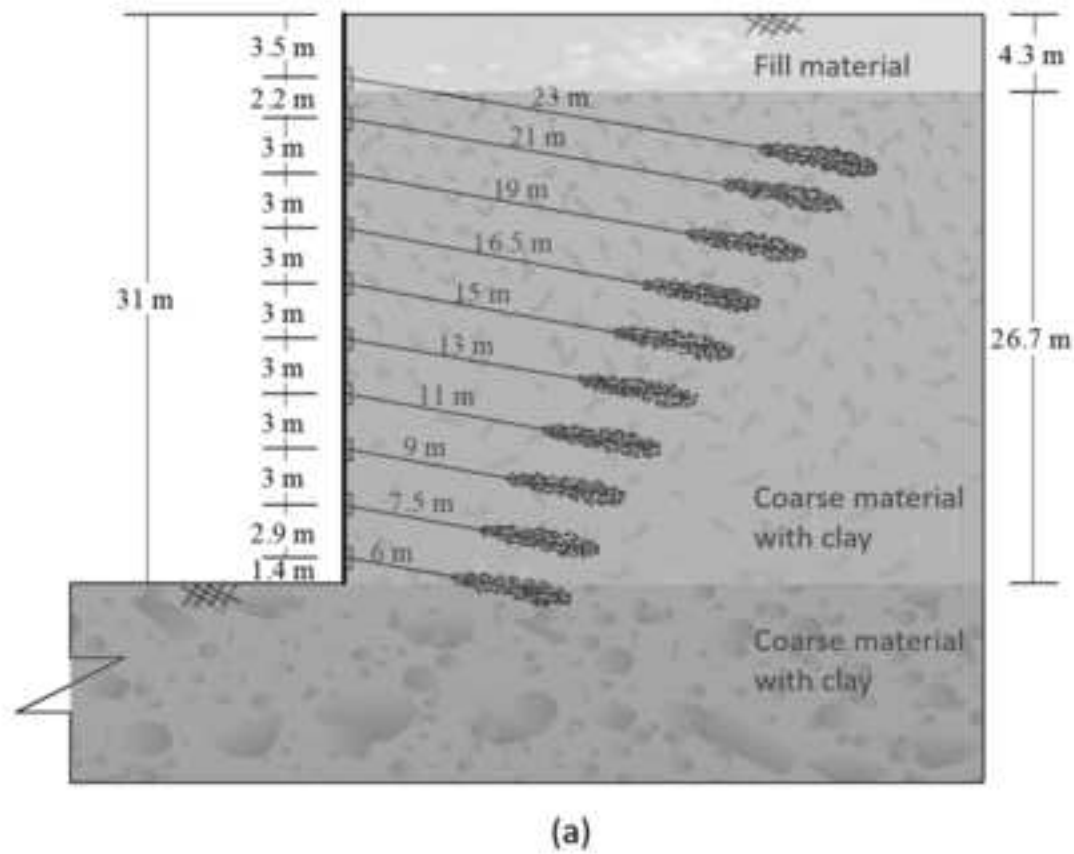
(d)

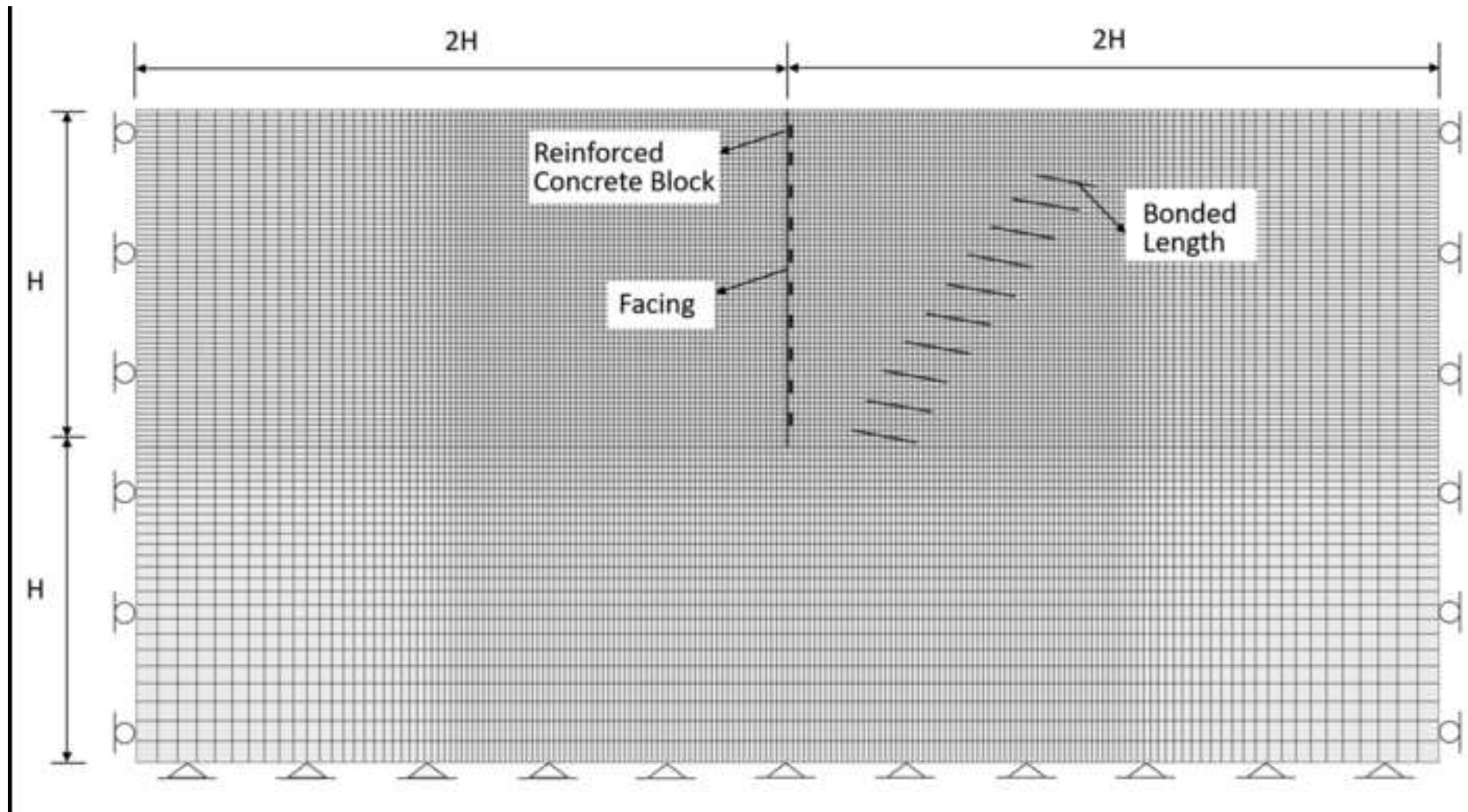


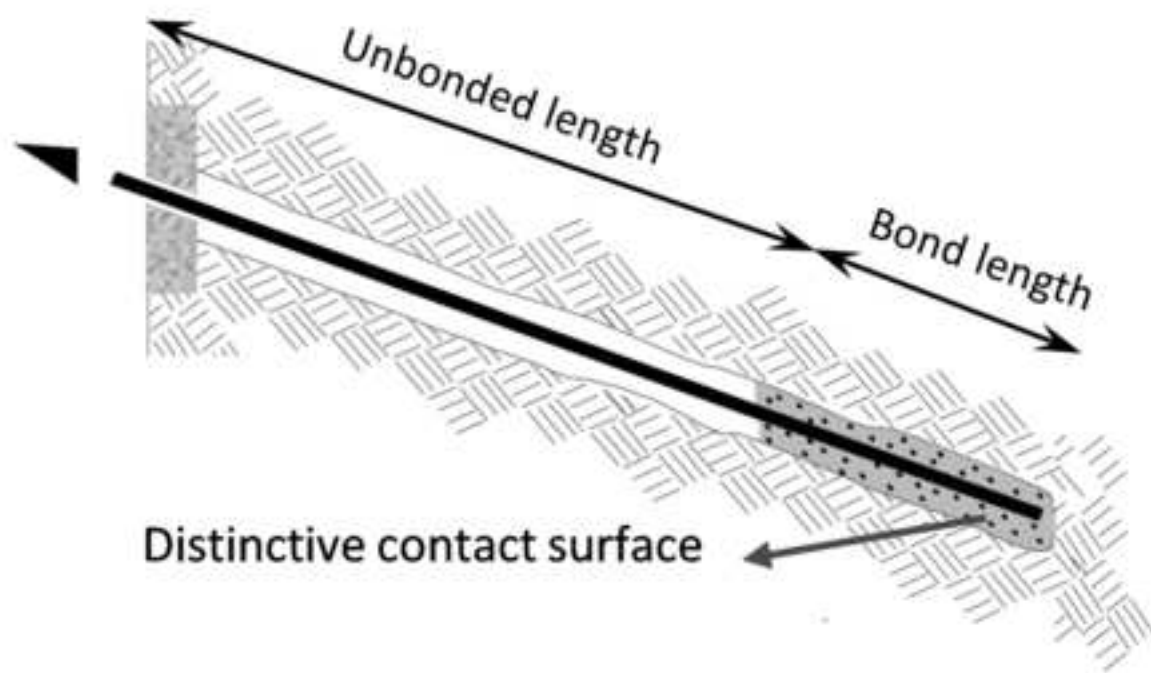
(a)



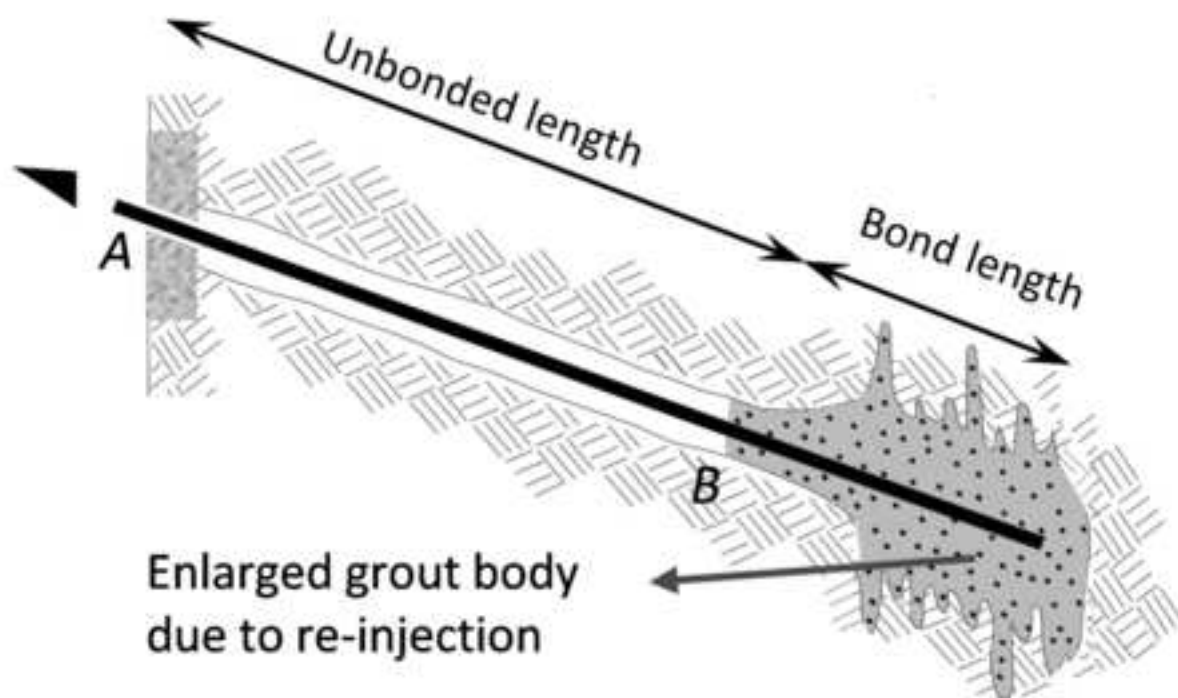
(b)



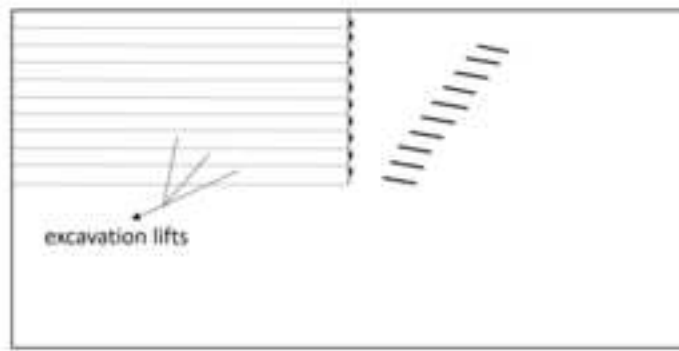




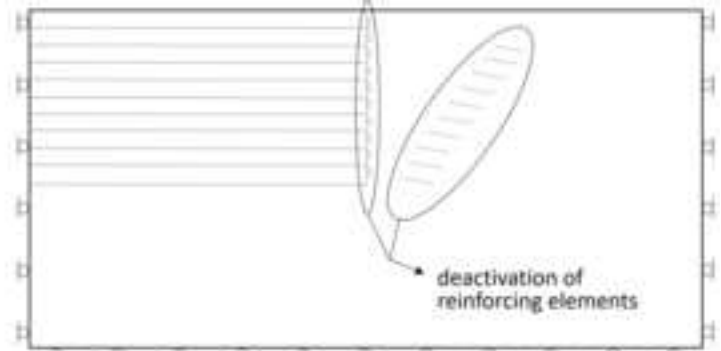
(a)



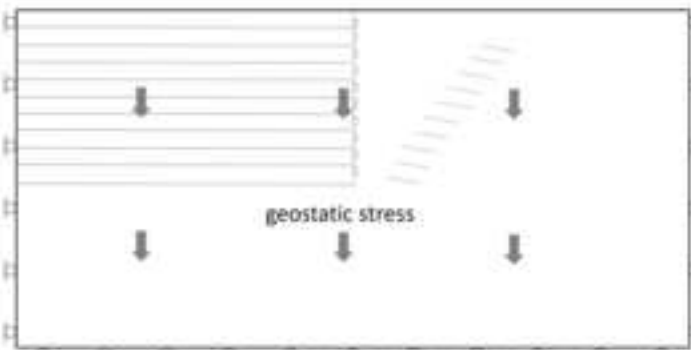
(b)



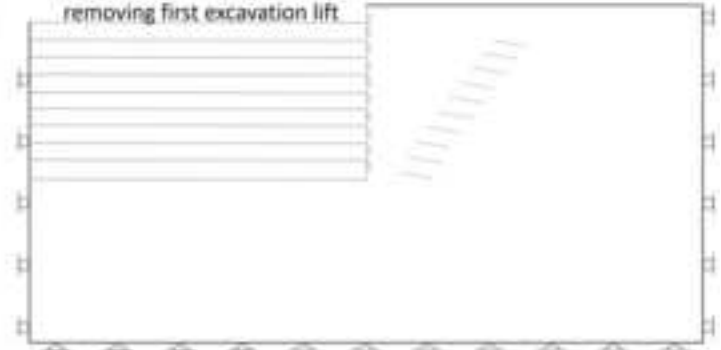
(a) Step 1



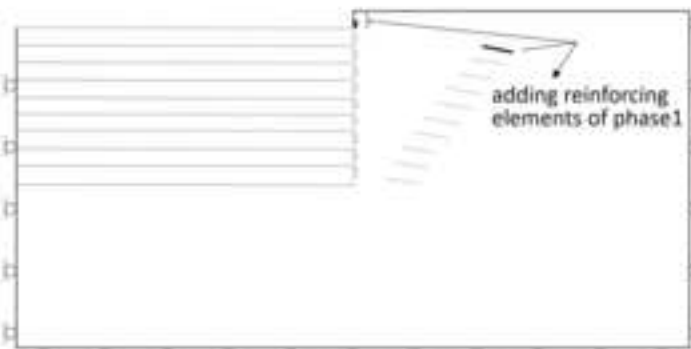
(b) Step 2



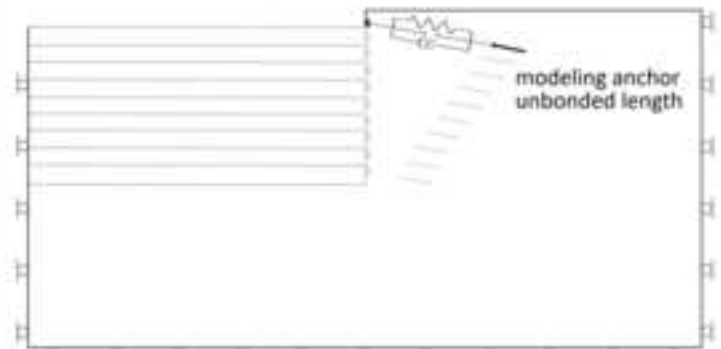
(c) Step 3



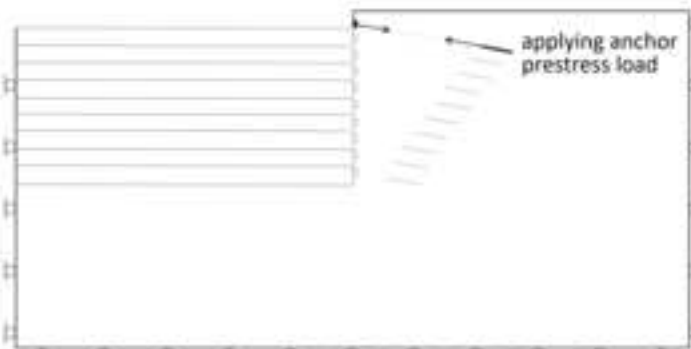
(d) Step 4



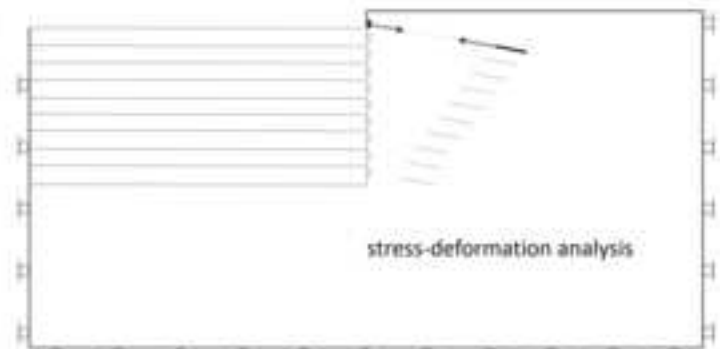
(e) Step 5



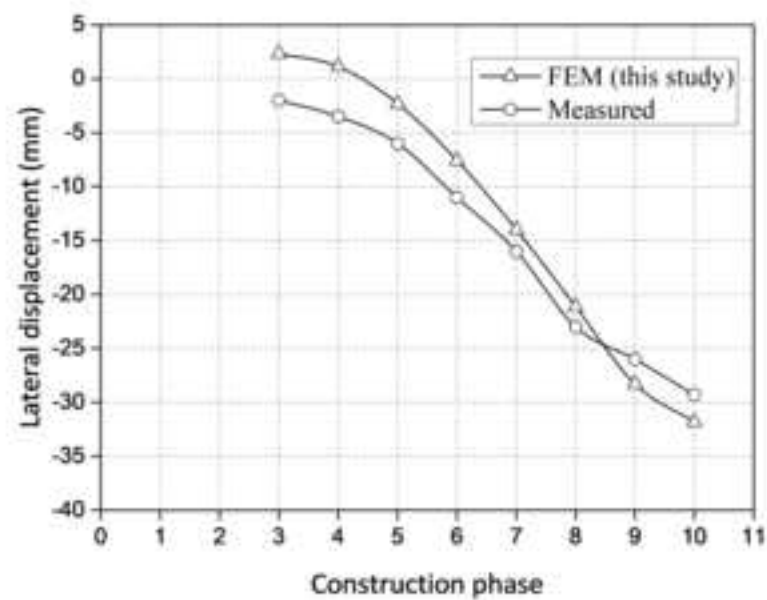
(f) Step 6



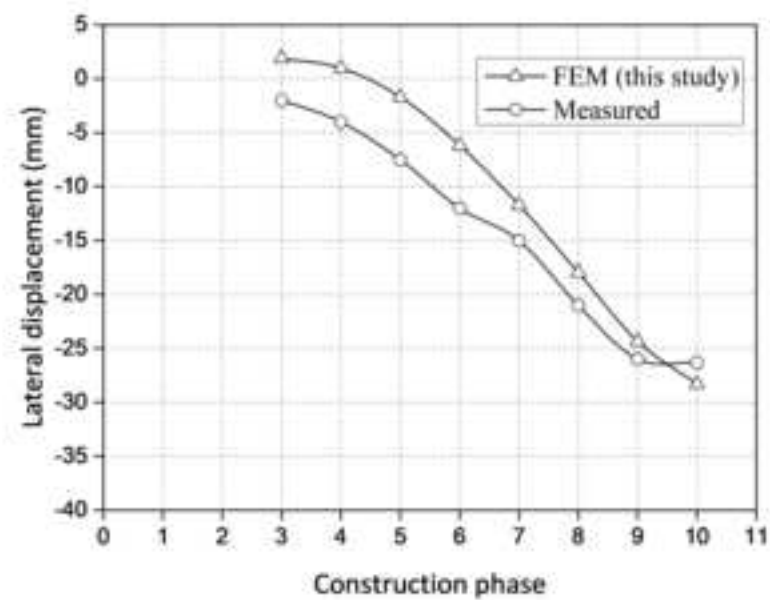
(g) Step 7



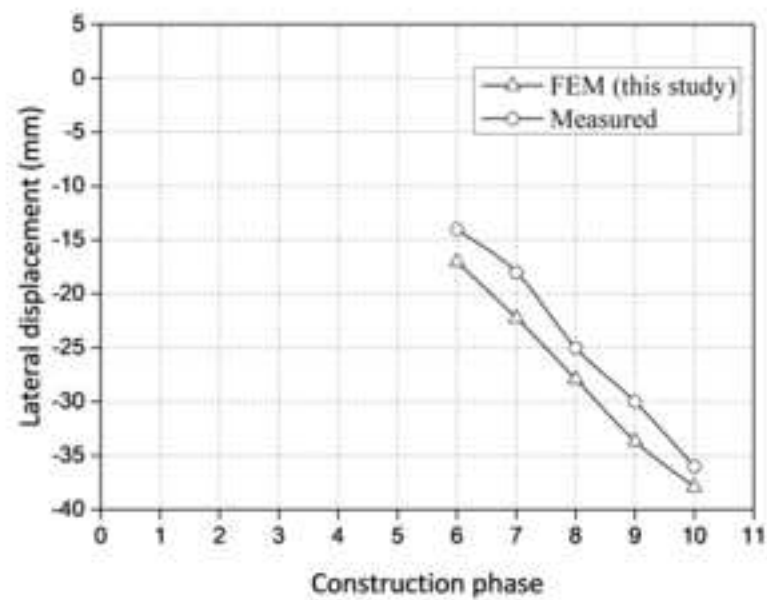
(h) Step 8



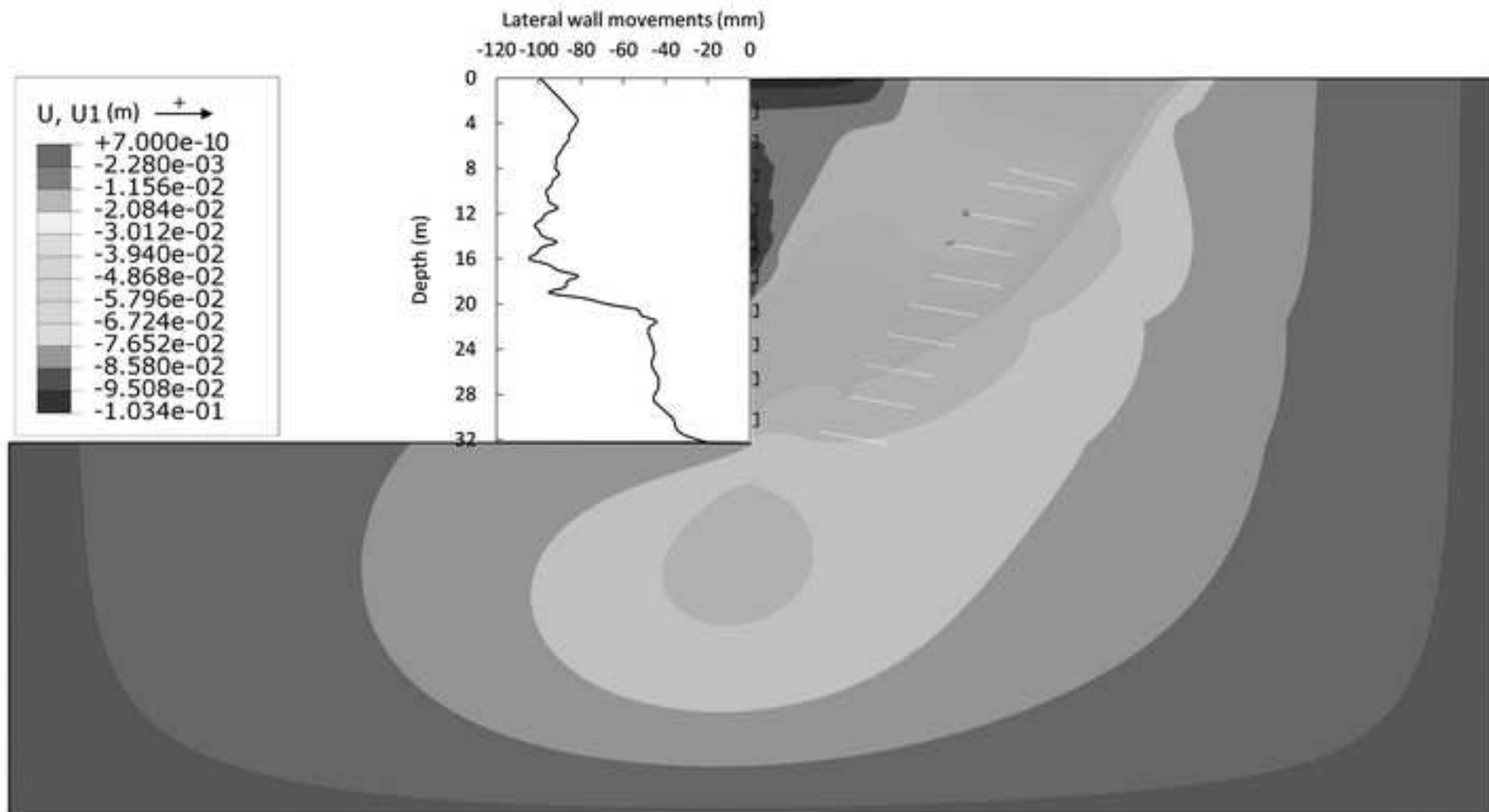
(a) Point NPA

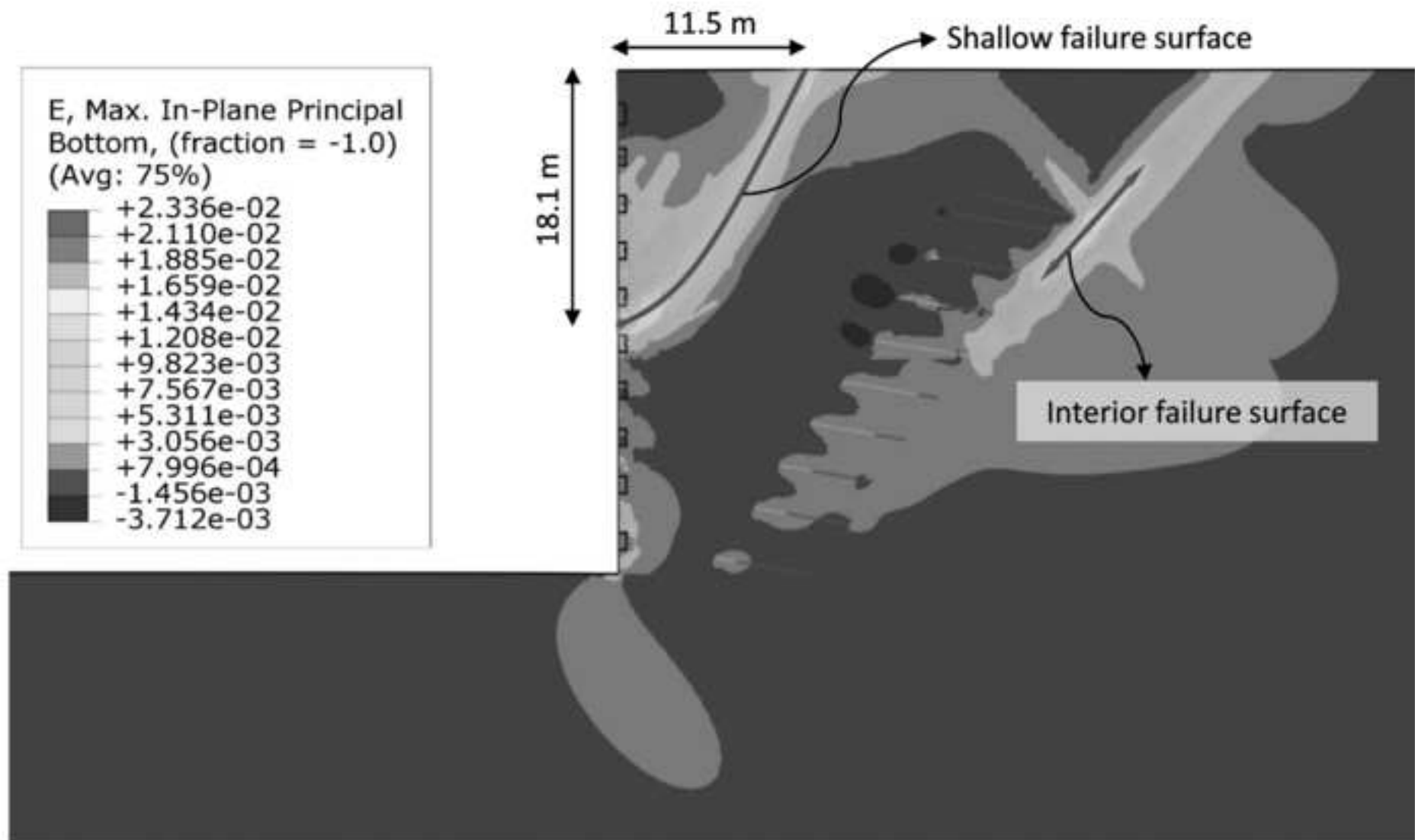


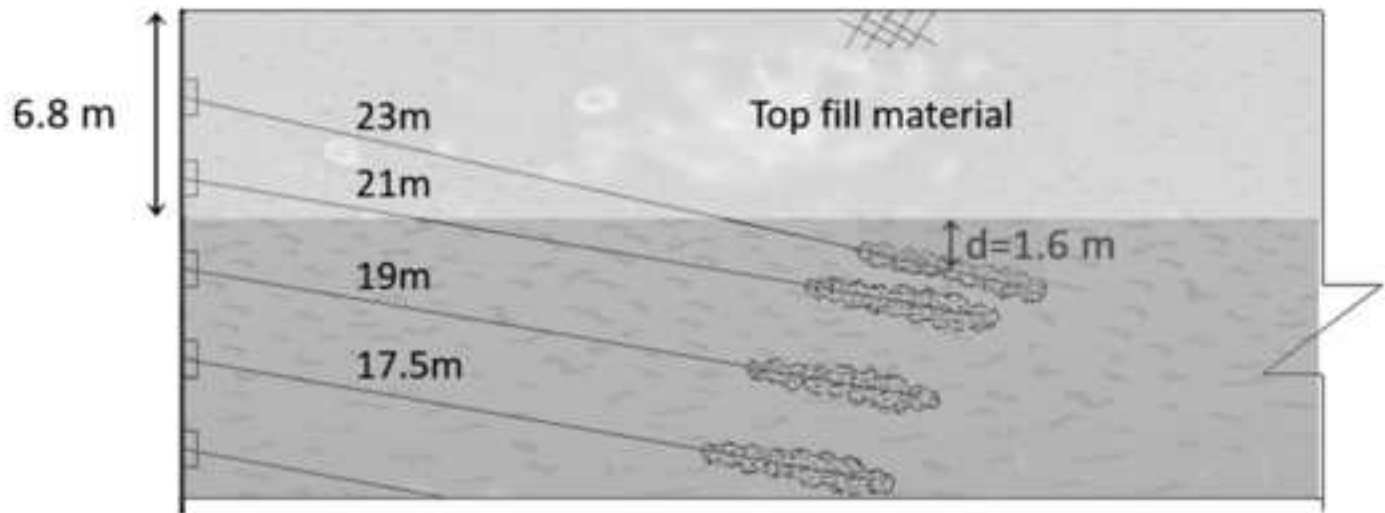
(b) Point NPB



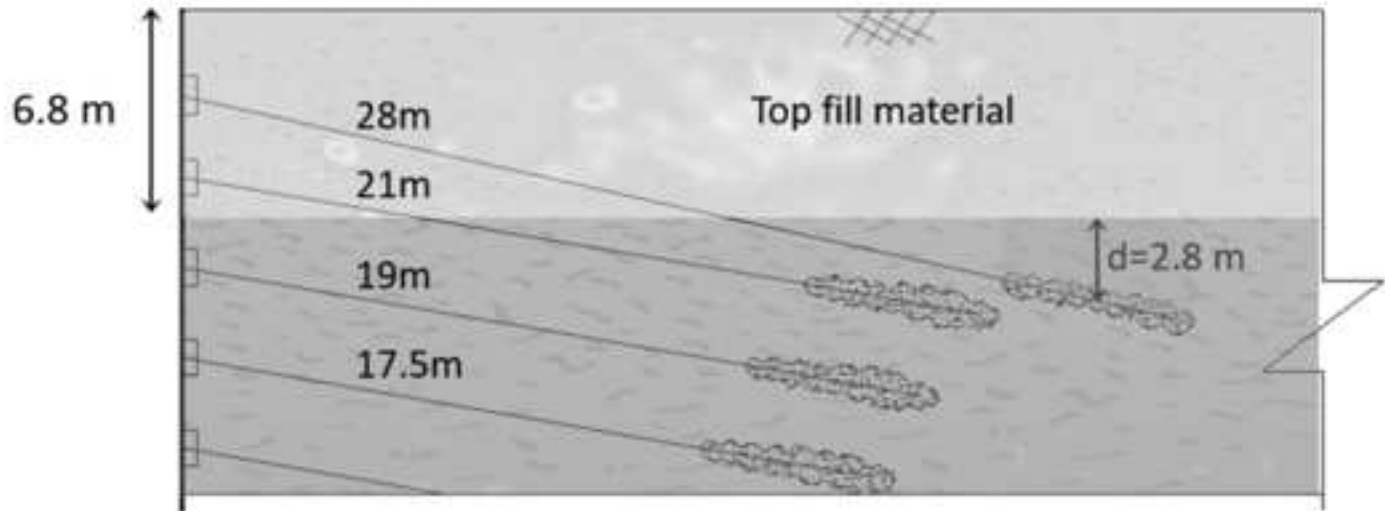
(c) Point NPC





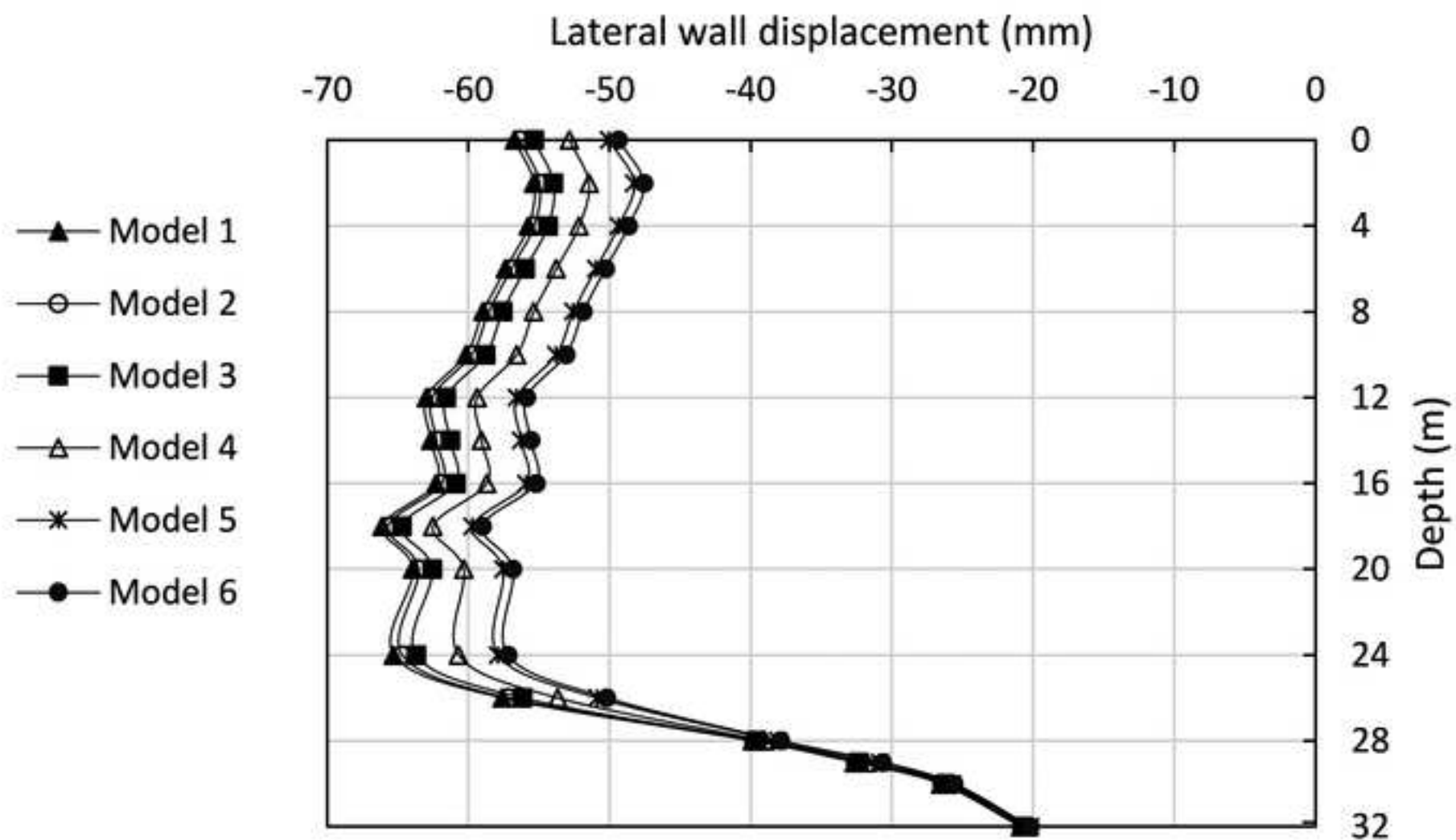


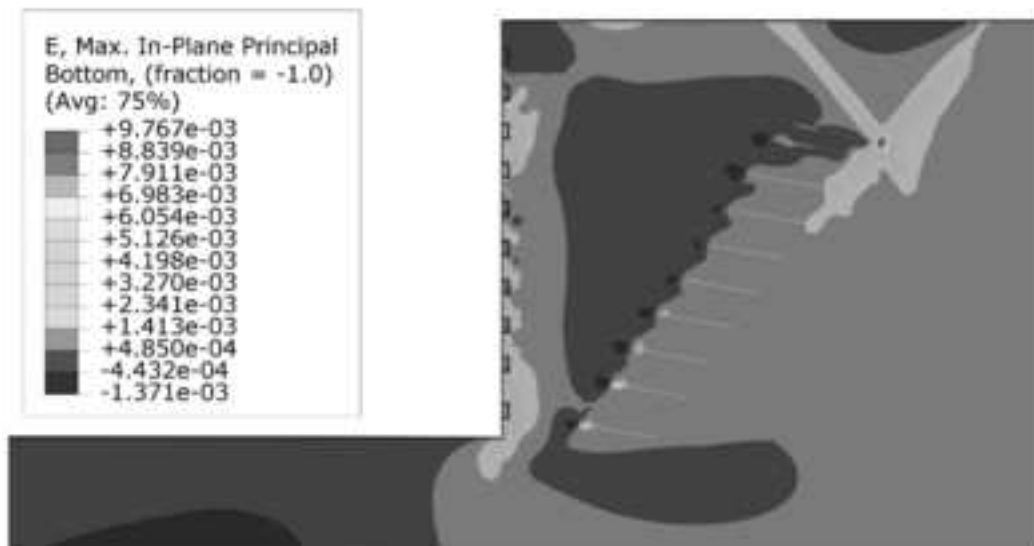
(a) Model 1



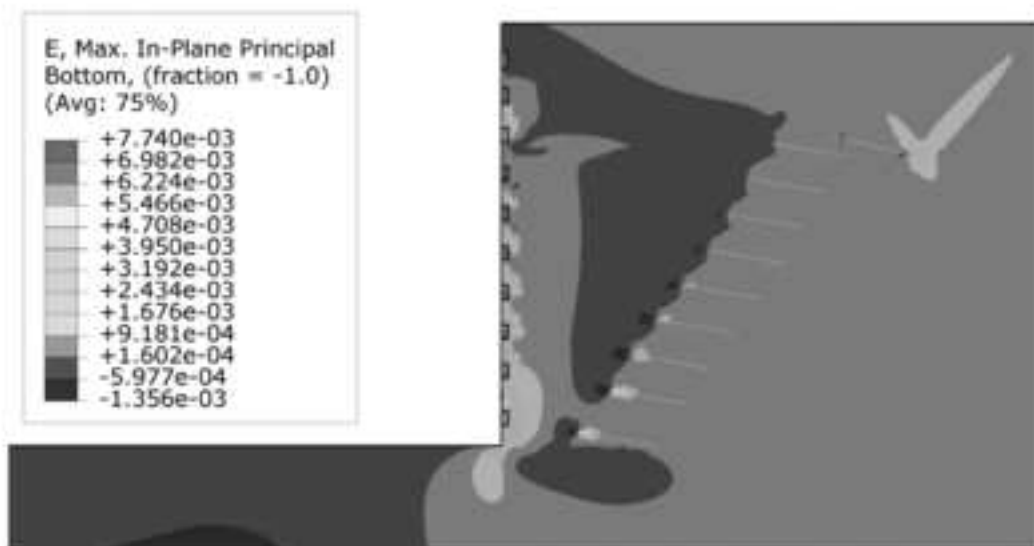
(b) Model 6

Note: d represents vertical distance between the center of the uppermost anchor bonded zone and top fill material

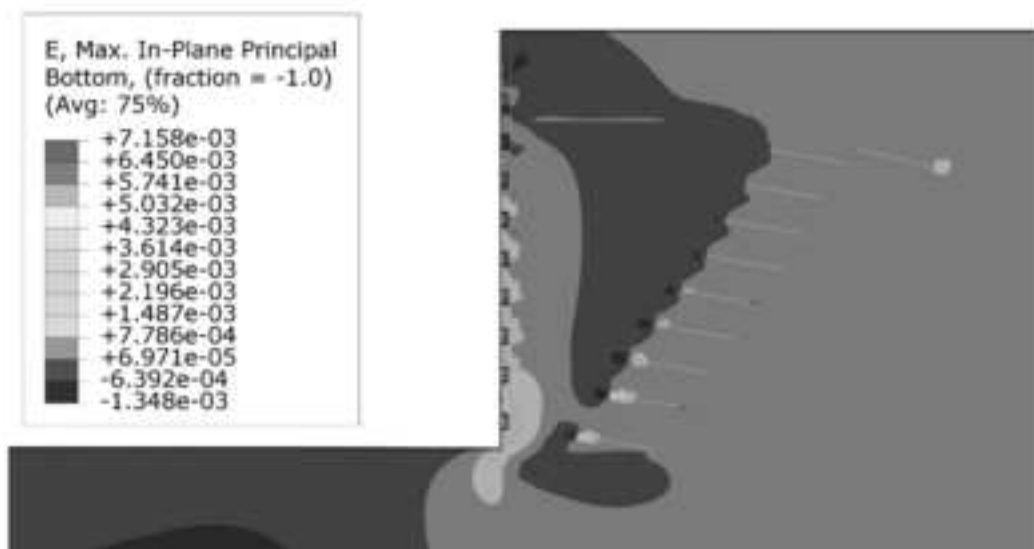




(a) Model 1



(b) Model 4



(c) Model 6

Table 1. Properties of reinforcing elements (S.E.S. Consulting & Contracting Co., 2013)

Element	ρ (kg/m ³)	E (GPa)	Poisson's ratio
Anchor bond length	2500	21	0.15
Anchor unbonded length	7800	210	0.3
Reinforced concrete block	2500	21	0.15
Facing	2400	21	0.15

Table 2. Geological characteristics of the alluvium formations in Tehran (Sharifzadeh et al., 2013)

Formation type (name)	Thickness (m)	Grain size description	Compaction
A (Hezardarreh)	>1000	Sandy gravel to gravelly sand, dipped bedding	High cemented
B (Kahrizak)	60	Sandy gravel to gravelly sand, boulders	Medium cemented
C (Tehran alluvial)	60	Sandy gravel to gravelly sand	Medium cemented
D (Recent alluvium)	<10	Sandy gravel to gravelly sand	Uncemented

Table 3. Geotechnical parameters of soil layers used in design (S.E.S. Consulting & Contracting Co., 2013)

Layer	Type	Geotechnical parameters					
		Υ (kN/m ³)	E' (MPa)	Poisson's ratio	c' (kPa)	φ' (deg)	Ψ (deg)
Top layer	Fill material	18	15	0.3	10	25	0
Middle layer	Coarse material with caly	21	80	0.3	40	40	0
Base layer	Coarse material with caly	21	125	0.3	100	40	0





